The Perceived Support From Light and Color Before and After an Evidence-Based Design Intervention in an Emergency Department

(article starts on next page)

Plant and system-level performance of combined heat and power plants equipped with different carbon capture technologies

Tharun Roshan Kumar [*], Johanna Beiron, Maximilian Biermann, Simon Harvey, Henrik Thunman

Division of Energy Technology, Department of Space, Earth, and Environment, Chalmers University of Technology, SE-412 96, Gothenburg, Sweden

HIGHLIGHTS

- Process modeling and integration of CCS technologies with respect to a reference bio-CHP plant.
- Key technology performance indicators for the carbon capture technologies are quantified.
- The possibility of integrating heat pumps into the BECCS plant is investigated.
- Case-specific exergy performance of the BECCS plant at the plant and DH system levels.
- BECCS plant with higher power preservation preferable from a local DH system perspective.

ARTICLE INFO

ABSTRACT

Installing carbon capture and storage (BECCS) capability at existing biomass-fired combined heat and power (bio-CHP) plants with substantial emissions of biogenic CO_2 could achieve significant quantities of the negative CO_2 emissions required to meet climate targets. However, it is unclear which CO_2 capture technology is optimal for extensive BECCS deployment in bio-CHP plants operating in district heating (DH) systems. This is in part due to inconsistent views regarding the perceived value of high-exergy energy carriers at the plant level and the extended energy system to which it belongs. This work evaluates how a bio-CHP plant in a DH system performs when equipped with CO_2 capture systems with inherently different exergy requirements per unit of CO_2 captured from the flue gases. The analysis is based upon steady-state process models of the steam cycle of an existing biomass-fired CHP plant as well as two chemical absorption-based CO_2 capture technologies that use hot potassium carbonate (HPC) and amine-based (monoethanolamine or MEA) solvents. The models were developed to quantify the plant energy and exergy performances, both at the plant and system levels. In addition, heat recovery from the CO_2 capture and conditioning units was considered, as well as the possibility of integrating large-scale heat pumps into the plant or using domestic heat pumps within the local DH system. The results show that the HPC process has more recoverable excess heat (~0.99 MJ/kg$CO_{2,captured}$) than the MEA process (0.58 MJ/ kg$CO_{2,captured}$) at temperature levels suitable for district heating, which is consistent with values reported in previous similar comparative studies. However, using energy performance within the plant boundary as a figure of merit is biased in favor of the HPC process. Considering heat and power, the energy efficiency of the bio-CHP plant fitted with HPC and MEA are estimated to be 90% and 76%, respectively. Whereas considering exergy performance within the plant boundary, the analysis emphasizes the significant advantage the amine-based capture process has over the HPC process. Higher exergy efficiency for the CHP plant with the MEA capture process (~35%) compared to the plant with the HPC process (~26%) implies a relatively superior ability of the plant to adapt its product output, i.e., heat and power production, and negative-CO_2 emissions. Furthermore, advanced amine solvents allow the BECCS plant to capture well beyond 90% of its total CO_2 emissions with relatively low increased specific heat demand.

* Corresponding author.

Nomenclature

Abbreviations

BECCS	Bio-energy with carbon capture and storage
bio-CHP	Biomass-fired combined heat and power
CAP	Chilled ammonia process
CC	Carbon capture
CCS	Carbon capture and storage
CDR	Carbon dioxide removal
CHP	Combined heat and power
CHPCC	Combined heat and power plant with stand-alone carbon capture plant
CHP-CCS	Combined heat and power plant with carbon capture, compression, and liquefaction units
CHP-HPC	CHP model integrated with the HPC model and CO_2 conditioning models
CHP-MEA	CHP model integrated with the MEA model and CO_2 conditioning models
CHP-MEA-HP	Large-scale heat pump integrated into the modeled CHP-MEA process
Cond. Drum	Condensation drum
COP	Coefficient of performance
DACCS	Direct air carbon capture and storage
DH	District heating
FGC	Flue gas condenser
GSHP	Ground source heat pump
HDD	Heat demand density (kWh/m^2)
HEX	Heat exchanger
HHV	Higher heating value (MJ/kg)
HP	High pressure
HPC	Hot potassium carbonate
IPCC	Intergovernmental Panel on Climate Change
LHV	Lower heating value (MJ/kg)
MEA	Monoethanolamine
PEN	Penalty
PP	Power preservation

REF	Reference
Solv.	Solvent
SRD	Specific reboiler duty

Symbols

CHP_{PP}	Power preservation in the bio-CHP plant with and without CCS units (P_{CHPCCS}/P_{REF})
$\dot{E}$	Exergy flow
$e_{j,ch}^0$	Standard chemical exergy of gas component
$\dot{m}$	Mass flow (kg/s)
P_{cc}	Electricity demand in the carbon capture and liquefaction units
P_{CHPCCS}	Net power delivered by the bio-CHP plant with CCS units
P_{REF}	Net power delivered by the reference bio-CHP plant without CCS units
Q	Heat duty (MW)
Q_{CC}	Steam demand in the carbon capture and liquefaction units
Q_{CHPCCS}	Net heat delivered by the bio-CHP plant with CCS units
$\dot{Q}_{fuel}$	Biomass fuel input to the bio-CHP plant
Q_{REF}	Net heat delivered by the reference bio-CHP plant without CCS units
R	Universal gas constant (8.3145 J/mol·K)
x	Mole fraction
α	Loading (mol/mol)

Subscripts

cfg	cleaned flue gas
ext-sys	extended system
fg	flue gas
liq	liquid
pen	penalty
q	heat flows
reb	reboiler
ref	reference
source	heat source (ground) for the heat pump at 10 °C
w	work

1. Introduction

Carbon dioxide removal (CDR) technologies, such as bioenergy carbon capture and storage (BECCS) and direct air carbon capture and storage (DACCS), are considered to be crucial climate change mitigation options. The recent Intergovernmental Panel on Climate Change (IPCC) Special Report [1] has projected that a BECCS deployment of up to 8 $GtCO_2$/yr by mid-century is needed to limit global warming to 1.5 °C. Accordingly, the Swedish climate goal of net-zero emissions by the Year 2045 [2] is expected to be complemented with a proposed target of 3–10 $MtCO_2$ of annual negative emissions via BECCS to compensate for hard-to-abate sector emissions. Existing biomass-fired combined heat and power (bio-CHP) plants, which are among the largest point-source emitters of biogenic CO_2 in Sweden, could be converted to large-scale CO_2 removal plants through the integration of carbon capture processes. A recent study that investigated the techno-economic potential of BECCS from waste and biomass-fired CHP plants (hereinafter referred to as 'bio-CHP' plants) in Sweden estimated a total potential for negative emissions of 10–16 $MtCO_2$ annually, corresponding to 24%–40% of Sweden's annual territorial fossil CO_2 emissions (roughly 40 $MtCO_2$) [3]. A recent study conducted by Fuss et al. [4] concluded that carbon capture would be required at all of the large-scale bio-CHP plants in Sweden to achieve the proposed Swedish BECCS target of 10 $MtCO_2$/yr by the Year 2045, assuming that the target is to be met by bio-CHP plants alone with their CO_2 capture units capturing 90% of their total biogenic emissions.

Bio-CHP plants in Sweden operate, in most cases, within a district heating (DH) system and are typically the primary providers of district heat in the region. One such plant is Stockholm Exergi's CHP8 plant, which is one of the world's largest bio-CHP plants, with a production capacity of 280 MW of district heat and 130 MW of electricity, supplying over 80% of the DH demand in Stockholm [5]. This bio-CHP plant was also recently awarded funding by the EU Innovation Fund for the demonstration and full-scale implementation of BECCS with a capture capacity of approximately 800 kt/yr of biogenic CO_2 [6]. However, retrofitting a CHP plant that operates in a DH system with CO_2 capture and conditioning units (hereinafter referred to as 'CCS units') is expected to incur an energy penalty on its overall energy efficiency. The extent and nature of the penalty will depend on the chosen CO_2 capture technology. Furthermore, such a retrofit will negatively affect the existing local energy system as it will have to compensate for the lost heat and power production.

Gustafsson et al. [7] have investigated and reported an energy penalty that ranges from −3% to + 7% for a planned full-scale integration of the hot potassium carbonate (HPC) CO_2 capture process into the CHP plant (CHP8) in Stockholm. The energy penalty represents the percentage change in the total useful energy output of the reference plant, i. e., heat and power production, with the integration of the CCS units. The partly negative span for the energy penalty, reported in [7], indicating a higher total energy output compared to the reference plant without CCS units, results from the assumption of slightly lower return (43 °C) and supply temperatures (78 °C) for the DH water flows, compared to the

average Swedish temperatures of 47 °C and 86 °C, respectively [8]. Similarly, the partly positive span of energy penalty reported by Gustafsson et al. [7] corresponds to the case in which higher district heating return (55 °C) and supply temperatures (110 °C) are considered. The HPC process was originally developed and used as a gas purification technology [9], and it has only been investigated in a few academic studies (summarized in the following paragraph) as a potential CO_2 capture process due to its relatively high specific power consumption (per tCO_2 captured), as compared to other amine-based capture technologies. The HPC process is, however, commercially offered as a carbon capture technology [10–12]. A high-power demand incurs a significant energy penalty in the context of fossil fuel power plants, which were the intended application in early CCS research and development. Furthermore, it is not realistic to recover waste heat in power plants due to the low-temperature level of such heat. Nevertheless, the HPC technology is promising in the context of a CHP plant operating in a district heat system, as argued by Levihn et al. [13].

A few recent studies have evaluated the performances of different CO_2 capture technologies retrofitted to CHP plants and waste-to-energy plants in a DH context [14,15]. For example, Djurberg R. [14] compared the HPC, monoethanolamine (MEA), and chilled ammonia (CAP) capture processes retrofitted to a CHP plant in Uppsala, assuming a 90% capture rate for the three capture technologies. They concluded that CAP is the economically feasible capture technology, followed by the MEA and HPC processes, considering waste heat from the CCS units is utilized for heating DH water. However, their work did not consider excess heat recovery from flue gas compression units in the HPC process, which could have led to an overestimation of the specific capture costs for the HPC process. Furthermore, previous work on CAP [16] highlighted that this capture technology is only applicable in regions that have access to low-temperature cooling water (~5°C) and for flue gas streams with a high CO_2 concentrations (>15 vol.% CO_2) to minimize the cost associated with ammonia slip control and utility costs. However, many CHP plants operating inland have limited access to cooling water at these low temperatures. In addition, experimental work [17] and process modeling studies [18–20] of the CAP process have shown that this capture process is limited up to a capture rate of 90%, due to increasing specific reboiler duty and increasing specific cooling requirements to avoid ammonia emissions in excess of 10 ppm [21]. These aforementioned limitations of CAP were not considered in the techno-economic assessment by Djurberg R. [14].

Several studies have evaluated the performance of a CHP plant equipped with a CO_2 capture unit, mainly applying the benchmark amine-based (MEA) solvent [22,23]. However, CO_2 capture processes with amine-based solvents are inherently different from the HPC process in that they do not require flue gas compression and have a higher heat demand per tonne of captured CO_2 to regenerate the rich-amine solvent (specific reboiler duty, SRD), which also results in a significant energy penalty for the CHP plant. Wide-ranging overall energy penalties are reported for an amine-based capture plant retrofitted to CHP plants evaluated in different contexts concerning their DH network and the regional market conditions. The differences are due to the very different technologies available to compensate for the loss of power and/or heat output from the CHP plant associated with implementing CCS. Pröll and Zerobin [22] have investigated large-scale BECCS at a bio-CHP plant with a maximum fuel capacity of 66 $MW_{th,LHV}$, and an amine-based post-combustion CO_2 capture technology and have found that it incurs energy penalties of about 40.7% and 36.1%, respectively, depending on whether conditioning of the captured CO_2 to pipeline specifications is considered or not. Similarly, Kärki et al. [23] have investigated amine-based CO_2 capture for a 1,020-$MW_{th,HHV}$ CHP plant and estimated the energy penalty to be approximately 16%. In general, these studies have been limited to one specific CO_2 capture technology applied to a CHP plant in a DH system. In some cases, the application of CCS at the CHP plant has been compared with other industrial CHP plants or dedicated electric power plants, such as condensing power plants or natural gas

combined cycle plants. Thus, it is crucial to evaluate different capture technologies integrated into a specific large-scale CHP plant that operates in its local DH system in order to highlight the various operational differences and the impacts that such integration has on both the CHP plant and the consumers of its energy services, i.e., primarily DH and power.

The amount of available excess heat that can be recovered from the capture and conditioning units and delivered to a DH network will depend on the type of CCS technology retrofitted to the CHP plant. For example, Eliasson et al. [24] have estimated that roughly 25% of the heat supplied to an amine-based capture plant can be recovered via direct heat exchange and delivered to a DH network. In contrast, the HPC process is expected to have a marginally higher heat recovery potential [7,14,15], mainly due to the heat that can be recovered from the flue gas compression section while incurring considerable losses to the electricity delivery capacity from a CHP plant. Hammar C. [15] quantified and compared the DH and electricity delivery losses for a waste-CHP plant equipped with MEA and HPC capture technologies. In comparison to the DH delivery from the waste-CHP plant without CO_2 capture, they concluded that the MEA process retains 99% of the DH delivery capacity, whereas the capacity increases by 7% for the HPC process due to the higher amount of recoverable excess heat from the CO_2 capture and liquefaction units. In addition, the electricity delivery losses related to the CHP plant without CO_2 capture, alternatively, the retained or preserved electric power production capacity with the integration of CCS units to the waste-CHP plant was estimated to be 80% and 56% for the MEA and HPC processes, respectively.

Eliasson et al. [25] have investigated different strategies to utilize available excess heat in industrial plants, such as an integrated steel mill, to achieve cost-optimal heat supply to the CCS plant and the DH network. Thus, incorporating the significant influence of seasonal variations on the availability of excess heat into the optimal design and operational mode of the capture plant. Similar seasonal variations are expected in a large-scale CHP plant operating within a DH network. As mentioned above, different exergy requirements of different types of capture technologies are expected to affect the operational flexibility of a CHP plant in different ways. Higher preservation of electric power production capacity for a BECCS plant implies higher availability of high-exergy energy carrier, i.e., electricity, which inherently confers flexibility to the BECCS plant in that it could strategically distribute the electricity to the grid or utilize it within the plant to prioritize DH delivery. For example, integrating a heat pump that would upgrade low-grade excess heat from a specific CO_2 capture technology and its conditioning units could alleviate operational inflexibility or even further enhance the operational flexibility of the CHP plant. For example, Abrami G. [26] has estimated that integrating a heat pump into a waste-fired CHP plant retrofitted with CCS units would increase the total district heat supply by 10% compared to the existing plant without these units. Further details on the use of a large-scale heat pump in combination with a CHP plant (without CCS) [27] and strategies available for the flexible operation of CHP plants can be found elsewhere [28,29].

District heating and system perspectives: One aspect often neglected in process-level technological comparisons of CCS capture technologies for CHP plants is the impact on the amount of heat delivered to the DH system. In the literature, comparative techno-economic analyses are often limited to the plant system boundary, i.e., adopting the perspective of investors in the CO_2 capture technology who are also the owners of the CHP plants that emit CO_2. For example, Kärki et al. [23] have reported that factors such as the electricity price and EU ETS carbon price are expected to be the dominant determinants of the viability of CCS from an investor's point of view. It was also highlighted in the same study [23] that the most-feasible CO_2 capture solution was when there was heat recovery from the CCS plant and when the CHP plant had the flexibility to operate in condensing mode so that it could respond to high electricity prices. Different CO_2 capture technologies could result in altered electric power outputs from the CHP-CCS plant,

which could be consumed within the plant through large-scale heat pumps or exported, depending on electricity prices. From the investor's perspective, it is clear that the optimal CO_2 capture technology is the one that minimizes the cost of implementation of BECCS or maximizes profit, factors that are dependent upon the market conditions of the local energy system in which the CHP plant operates.

In Sweden, bio-CHP plants are one of the primary providers of DH. Since they operate in a closed DH market, they are regarded as local natural monopolies [30,31]. Thus, there are minimal limitations (apart from operational limitations such as minimum turbine load or power-to-heat ratio, as stated by Gustafsson et al. for the CHP8 plant [7]) on their electric power production levels, which are rather dependent upon the seasonal heating and cooling demands [27]. In this context, it is not clear how to select the optimal end-use of the high-exergy energy carrier, i.e., the low-carbon electricity generated by the CHP-CCS plant. While the low-carbon electricity could be generated and consumed cost-optimally by the energy-service provider, i.e., by the bio-CHP plant within its plant boundaries, the consumers of the low-carbon electricity could assign a higher value to the electricity due to its greater utility. More specifically, the generated electric power could be consumed in the local DH system to meet consumers' heating needs using decentralized domestic heat pumps. However, such power-to-heat technologies that compete with DH are hindered by pre-existing market entry barriers, as discussed by Åberg et al. [32]. The DH providers typically use pricing mechanisms to compete with decentralized heat pumps in the DH network [31,33]. In addition, the tax imposed on electricity [34] disincentivizes the use of electricity for decentralized heat production and dissuades consumers from installing domestic heat pumps, such as ground source heat pumps (GSHPs) or air-to-water heat pumps, instead of connecting to the DH grid, thereby reducing the overall DH system costs. Therefore, the perspectives of the energy service provider and the consumer are discrepant, and it is unclear as to what the optimal choice of CO_2 capture technology for a CHP-CCS plant would be, since the energy penalty incurred by the two capture technologies discussed above is either in the form of loss of heat or electric power production capacity. Furthermore, comparative studies of CO_2 capture technologies could result in different conclusions depending on the chosen system boundary and whether energy or exergy is used as a figure of merit.

Biermann M. [35] argued that specific conditions such as site-related conditions, policy landscape, product, and market-related factors could motivate partial capture in the process industry, where only a portion of the total on-site emissions are captured in CO_2 capture units. However, if large-scale negative-CO_2 emissions are to be achieved, bio-CHP plants require a CO_2 capture technology that not only incurs minimal energy penalty but also has the potential to go well beyond the '90%-capture rate', previously considered as the techno-economic limit of post-combustion CO_2 capture. Both pilot plant tests [36] and techno-economic studies [37–39] of the amine-based capture process in the literature have established that capture rates up to 99% can be achieved with a marginal increase in specific CO_2 capture costs. However, the possibility of a capture rate higher than 90% does not hold for both the CAP and the HPC processes without incurring a substantial increase in operational costs. For example, CAP pilot plant tests at different scales have shown an average capture rate of 75–85% [17], where increased capture rates eventually lead to higher ammonia slip [40], thereby leading to higher costs associated with controlling ammonia emissions [21]. For these reasons, CAP was not considered in this work. In contrast, the HPC process with a relatively harmless capture solvent requires significantly higher operating pressures and, thereby, higher electricity consumption to achieve a capture rate beyond 90%. Therefore, the HPC process was considered over the chilled ammonia process due to its lower environmental impact [41,42] and recoverable excess heat at higher temperatures that could be recovered for district heating. In line with the recommendations in Gustafsson et. al [7], the comparison of HPC process with MEA process, and the possibility of integrating heat pumps to recover more heat from the BECCS plants was considered

in this work.

This work presents a detailed comparison of CO_2 capture technologies not only as stand-alone technological options but also considering the impact on a process level within the existing bio-CHP plant boundaries, as well as its DH system. The results indicate the optimal CO_2 capture technology for different system boundaries. More specifically, this work presents a detailed comparison of the HPC capture process (as considered for planned full-scale implementation [43] by Stockholm Exergi) and the MEA capture process (i.e., a first-generation amine solvent commonly considered as the benchmark solvent in the literature) in the context of a reference bio-CHP plant in a DH system. Although advanced amine-based solvents could incur relatively lower SRD at a 90% capture rate or have capture rates > 90% with minimal increase in SRD compared to the benchmark MEA solvent, this work intentionally adopts a conservative approach. The MEA capture process is therefore compared with the HPC process at the standard 90%-capture rate to clearly establish the optimal CO_2 capture technology at the same absolute amount of CO_2 captured from bio-CHP plants. To this end, this work contributes with a simplified method to evaluate BECCS systems in a DH system and presents the consequence of using energy or exergy as the figure of merit for different system boundaries.

Specifically, the work seeks to:

1. compile technical performance data for the HPC and MEA capture processes at the technology level with a design capture rate of 90% (stand-alone processes),
2. evaluate the exergy and energy performances of the two CO_2 capture processes within the boundary of a CHP-CCS plant, i.e., at the process level,
3. assess at the system level the exergy and energy performances of CHP-CCS plants that are retrofitted with either the MEA (CHP-MEA) or HPC (CHP-HPC) capture technology. This analysis includes the CHP plant, as well as the consumers of the energy services that the CHP plant provides via the local DH system and the electricity grid,
4. compare the local DH system with CHP-CCS plants that include electricity-driven heat pumps at two different locations: 1) centralized heat pumps, i.e., large heat pumps that can upgrade residual heat from the capture plant and deliver it to the DH grid; and 2) decentralized heat pumps that use the ground as the heat source (GSHPs) to meet the end-use energy needs within the local DH system, i.e., primarily space heating and domestic hot water

The method (Section 2), results (Section 3), and discussion (Section 4) sections of the paper follow the same structure as the specific objectives presented above with – i) technological comparison of CO_2 capture technologies as a stand-alone process, followed by ii) comparison of CHP-CCS plant cases within its plant boundaries, and, iii) within its extended system boundary, i.e., the local DH system.

2. Method

Fig. 1 shows an overview of the method used in this work, together with the two system boundaries: 1) the *CHP-CCS plant boundary*, which includes the bio-CHP plant fitted with CO_2 capture and conditioning (CO_2 compression and liquefaction for ship transport) units; and 2) the *extended system boundary*, which includes the local DH system, where it is assumed that the electric power delivered by the bio-CHP plant is consumed by decentralized ground source heat pumps (GSHPs) installed to meet the indoor-climate needs of end-users in residential buildings. The two system boundaries are chosen to allow evaluations of the plant- and system-level performances of a reference bio-CHP plant that is retrofitted with different carbon capture technologies. The comparison of the two carbon capture technologies is performed for a large-scale reference bio-CHP plant operated by Stockholm Exergi [6] in Stockholm, Sweden. Table 1 shows the relevant data for the reference bio-CHP plant. A steady-state model of the reference bio-CHP plant was
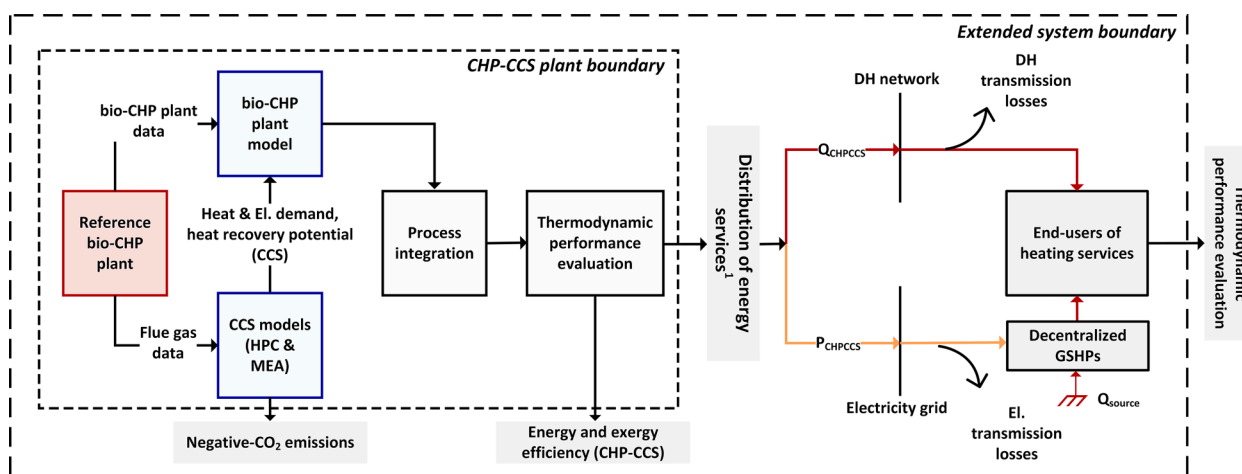
Fig. 1. Overview of the methods and models used with the two system boundaries. bio-CHP plant boundaries; and the extended system boundary (the local DH system). The reference bio-CHP plant (indicated in red) data are fed to the developed numeric models, indicated in blue. Finally, the applied methods and results obtained are highlighted in gray. [1]Delivered energy services of the bio-CHP plant integrated with CCS (CHP-CCS), which includes the net district heating (DH) and power delivered to the bio-CHP plant's local DH system. Note that the delivered electricity to the grid is assumed to be consumed in decentralized GSHPs to meet indoor-climate needs, i.e., domestic hot water and space heating. (For interpretation of the references to colour in this figure legend, the reader is referred to the web version of this article.)

Table 1
Reference bio-CHP plant data [7].

Parameter	Unit	Value
Fuel type	–	Wood chips with 50% moisture content
Fuel input (lower heating value, LHV)	MW	362.1
Fuel input (higher heating value, HHV)	MW	451.1
District heat production capacity	MW	280
Electric power production capacity	MW	130
Live Steam temperature	°C	558.0
Live Steam pressure	bar	136.0
Flue gas flow rate	kg/s	174.2
Wet flue gas composition		
CO_2	vol.%	16.0
O_2	vol.%	3.2
H_2O	vol.%	5.3
N_2 and inert gases	vol.%	75.5

developed in EBSILON Professional with available plant data, and the MEA and HPC capture processes were modeled (steady-state) in Aspen Plus V12.1 and simulated with the reported flue gas data (see Table 1). The detailed modeling and validation of the bio-CHP plant and the carbon capture models are described in Section 2.1.

The heat and power demands of the two CO_2 capture plants were estimated using the capture plant models and thereafter used as inputs to the bio-CHP plant model so as to represent a bio-CHP plant retrofitted with the CCS units. The reference bio-CHP plant retrofitted with CCS units is referred to as a 'CHP-CCS plant' hereinafter. Pinch analysis, which is an energy-targeting method [44], was used to quantify the recoverable process heat from the two carbon capture processes assuming a minimum temperature difference of 5 °C for heat exchange with the DH water. The recoverable process heat is categorized as low-grade (47°–61 °C) or high-grade (61°–86 °C) heat, which is adapted from the generic Swedish DH system defined by Gustafsson et al. [7], with annual average representative temperature levels of 86 °C (supply) and 47 °C (return) [8]. Key performance indicators associated with the plant performance are then quantified for the CHP-CCS plants (CHP-

MEA and CHP-HPC) within the CHP-CCS plant boundary.

An extended system boundary is adopted to enable a fair comparison of the two CO_2 capture processes at the system level (see Fig. 1), which includes the bio-CHP plant and the end-users of the distributed energy service. Since DH is the primary energy service provided by the bio-CHP plant, we assume that GSHPs are used on the demand side to convert the delivered power to end-use heat, so as to meet the indoor-climate needs related to space heating and domestic hot water. This assumption mainly holds for regions in which DH and GSHPs compete or regions where the DH network does not benefit from a technological monopoly, as defined by Åberg et al. [32]. It is worth noting that air-to-water heat pumps could be an alternative solution with performance levels similar to those of GSHPs [45]. However, such heat pumps are not considered in this work due to their susceptibility to variable performance with variations in the outdoor temperature. This somewhat simplifies the analyses performed within the extended system boundary. Within the extended system boundary, the energy and exergy efficiencies are estimated, assuming an end-use energy temperature range of 30°–60 °C, for the supply of space heating and domestic hot water, respectively. Thus, the extended system boundary shown in Fig. 1 includes the transmission losses within the DH network and the electricity grid, as well as the conversion losses associated with the technical systems (e.g., GSHPs) used to meet the indoor-climate needs.

2.1. Model descriptions

2.1.1. Descriptions of the CO_2 capture and conditioning processes

Fig. 2 shows the process flowsheets of the two CO_2 capture processes. Both capture process simulation models in Aspen Plus V12 adopt rigorous rate-based models with detailed reaction kinetics. The mass transfer coefficients and interfacial areas in the packings were predicted using the correlations described by Bravo et al. [46], whereas the liquid holdup was estimated using the correlations reported by Stichlmair et al. [47]. Heat transfer coefficients were estimated via the Chilton and Colburn analogy [48]. The specifications of the CHP flue gas fed to the two CO_2 capture processes were taken from Gustafsson et al. [7] (see Table 1), with a flow of 174.2 kg/s, at ambient pressure and a temperature of 160 °C with a CO_2 concentration of 16 vol.%$_{wet}$ (as compared to coal combustion with ∼ 13 vol.%$_{wet}$). The two capture models' key assumptions and process parameters are compared in Table 2. The source of data presented in these Table 2 is based on previous work, mainly
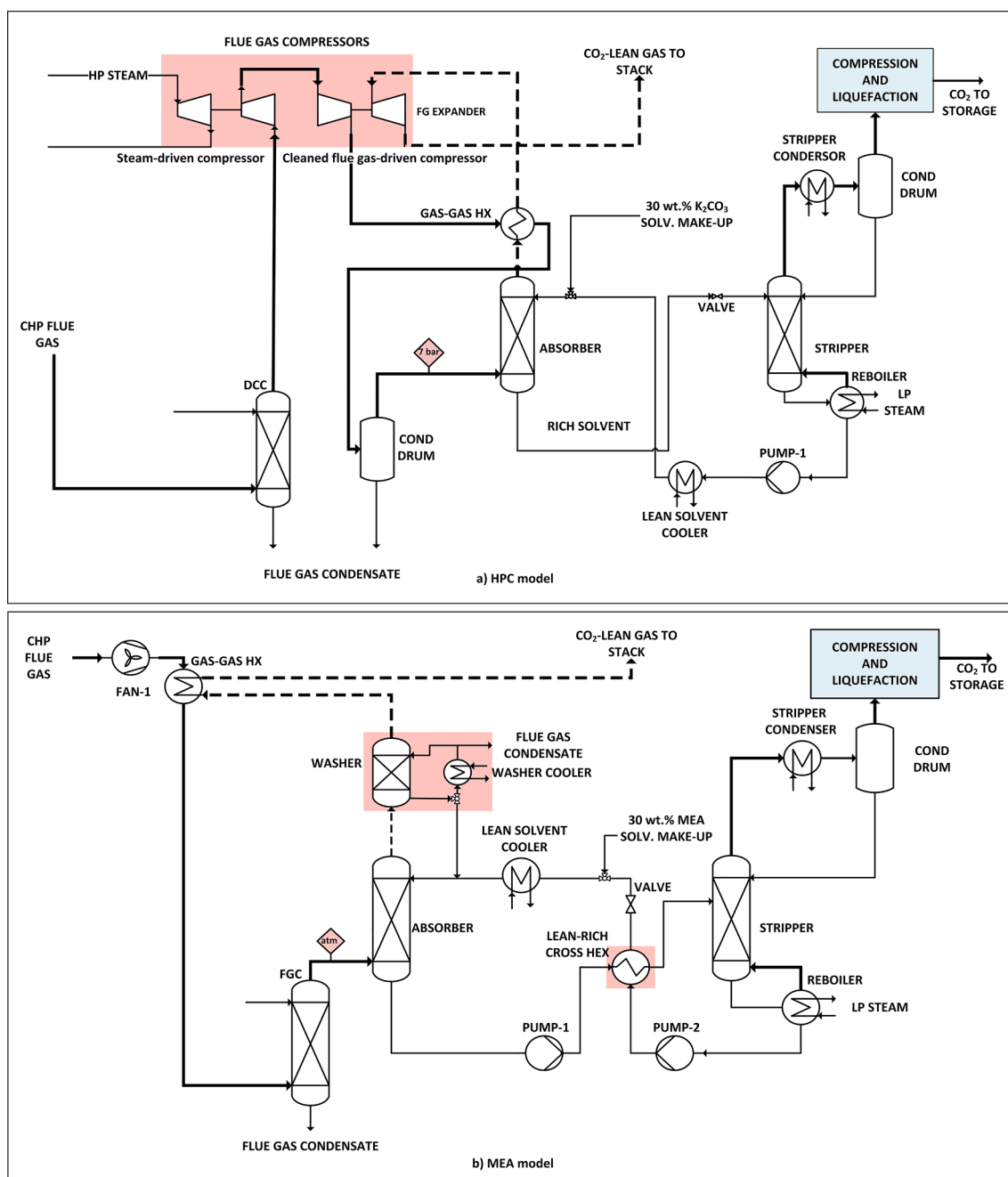
Fig. 2. Process flowsheet diagrams of a) the hot potassium carbonate (HPC) capture process; and b) the MEA capture process. The main differences between the two processes, i.e., the flue gas compression train in the HPC process and the cross-heat exchanger in the MEA process, are highlighted in the red-shaded areas. The CO_2 compression and liquefaction processes are common to both carbon capture models and therefore are highlighted in blue. Dashed lines depict the CO_2-depleted flue gas streams. Thick and thin solid lines depict the gaseous and liquid (solvent and water) streams, respectively. (Abbreviations. Lean-Rich Cross HEX–heat exchanger for the CO_2-rich and lean solvent, cond drum–condensation drum, FGC–flue gas condenser, HP – high pressure, Solv. – solvent). (For interpretation of the references to colour in this figure legend, the reader is referred to the web version of this article.)

Gustafsson et al. [7], for the HPC model and Biermann et al. [49,50], for the MEA model to obtain comparable results with the literature. Although the two simulation models were developed separately, necessary modifications were made to ensure design parameters and assumptions, e.g., capture rate, adiabatic and mechanical efficiencies, and column heights, are kept consistent to allow for a reasonable comparison.

The fundamental differences between the HPC and MEA process models include: (1) flue gas compression to allow the HPC to enhance the physical absorption of CO_2 in the absorber; (2) a cross-heat exchanger for the MEA process model, which was omitted in the HPC model to avoid modeling complexity, as the rich and lean solvents are typically at different pressures; alternatively, heat exchangers are used to recover heat from the lean solvent that is pumped back to the absorber from the stripper; (3) a washer unit, which is not considered for the HPC solvent owing to its much lower solvent volatility and water evaporation at higher pressures; and (4) the optimal stripper pressure (minimum SRD) in the HPC process is lower than in the MEA process, and this influences the reboiler temperature.

The MEA model assumes an aqueous solution of MEA at a concentration of 30 wt.%. The model was based on previous work conducted by Garðarsdóttir et al. [18] and Biermann et al. [50]. It was further

Table 2

Summary of the key process parameters and assumptions for the MEA and HPC CO_2 capture process models.

Parameter	MEA	HPC	Comment/Reference
Capture section			
Thermodynamic Properties	ENRTL-RK	ELECNRTL	MEA [49,50], HPC [7]
Lean solvent composition	30 wt.% MEA in H_2O	30 wt.% K_2CO_3 in H_2O	MEA [49,50], HPC [7,57,58]
CO_2 capture rate[1] (%)	90	90	Note that a conservative approach is taken here with the benchmark MEA solvent. Advanced amine solvents have achieved higher capture rates (>90%) with a similar range of SRD [36]
Isentropic efficiency (pumps, compressors, and gas expander)[2] (%)	85	85	
Mechanical efficiency (pumps, compressors, and gas expander)[2] (%)	95	95	
Flue gas fan/compressor discharge pressure[1] (bar)	1.16	7	[7,49,50]
Absorber gas outlet pressure[1] (bar)	1.06	7	[7,49,50]
Absorber gas inlet temperature[2] (°C)	42.5	42.5	Set to a constant value (taken from [7])
Absorber lean solvent inlet temperature[2] (°C)	42.5	42.5	Set to a constant value in both models for comparable results [49]
Direct contact cooler height[1,2] (m)	7	7	
Absorber packing height[1,2] (m)	20	20	Design factor (flooding approach set to 80%) for estimating the column diameter [49,50]
Water wash packing height[1] (m)	2	–	Included in the MEA model with its diameter equal to the estimated absorber diameter [49,50]
Stripper packing height[1,2] (m)	10	10	Design factor (flooding approach set to 80%) for estimating the column diameter [49,50]
Stripper outlet pressure[1] (bar)	1.9	1.2	MEA [49,50], HPC [7]
Stripper CO_2 gas outlet temperature (condenser temperature)[2] (°C)	20	20	
Minimum temperature difference (ΔT_{min}) in heat exchangers[2] (°C)	10	10	
Minimum temperature difference (ΔT_{min}) in stripper reboiler[2] (°C)	5	5	

[1]Constant design parameter.

[2]Assumptions made to ensure comparable results from both CO_2 capture models.

developed regarding the MEA chemistry, and reaction sets based on the most recent version of the MEA model by AspenTech [51], which has validated the model performance against pilot data by Notz et al. [52]. The updated model has also been validated against large-scale pilot data derived from testing CO_2 capture from a steam reformer flue gas [49,53]. Note that the property method ENRTL was used with the Redlich-Kwong equation of state for the vapor phase, instead of the PC-SAFT correlation, which is applied in the model developed by Aspen-Tech [51]. This was done to enhance convergence and entailed only minor deviations in SRD (<0.3%). The reaction sets for the absorber and

stripper were set up according to Zhang and Chen [54], incorporating the kinetic parameters described by Pinsent et al. [55] and Hikita et al. [56].

The HPC model assumes a solution that contains 30 wt.% aqueous potassium carbonate (K_2CO_3) as the capture solvent. This is considered to be the optimal solvent composition [57], being limited by a high solvent regeneration duty and salt precipitation in the lower and upper limits of the range for a 20–40 wt.% K_2CO_3 solution [57,58]. The operating conditions of the HPC model (Table 2) were chosen based on the work of Gustafsson et al. [7], in which an equilibrium-stage model of a full-scale capture plant (~90% capture rate) was developed using data obtained from a pilot-scale plant tested at the reference bio-CHP plant (CHP8). In the present work, however, a rigorous rate-based model was developed that utilizes the ELECNRTL property method in Aspen Plus [59], with its associated reaction sets, as described by Ayittey et al. [60], implemented with equilibrium and kinetic constants derived from AspenTech and Wu et al. [61,62]. The HPC model developed in this work was compared with published data from the full-scale models developed by Gustafsson et al. [7], based on their HPC carbon capture test plant data, and was validated with respect to the solvent loading capacity and the corresponding SRD. The reaction set list and model validation are provided in Supplementary Materials S.1.

The CO_2 compression and liquefaction processes were modeled based on the work carried out by Deng et al. [63], where the captured CO_2 stream from the two different CO_2 capture models was matched to the gas fed to compression and liquefaction train. This concentrated CO_2 stream from the capture models was assumed to consist only of CO_2, H_2O, N_2, and O_2 (and trace amounts of MEA in the stream from the MEA model; no significant traces of K_2CO_3 are carried over in the HPC model). This stream undergoes a three-stage intercooled compression process in the CO_2 compression train to attain the pressure required for liquefaction. The flue gas compression train was modeled with three compression stages with a constant pressure ratio per stage, increasing the pressure to 27.5 bar based on the specifications described by Deng et al. [63], which assume some level of impurities that requires flashing and purging [31]. Thus, the compression outlet pressure is higher than the delivery pressure. Although we did not resolve these impurities in our model, we included the elevated pressure to obtain a conservative estimate of the level of power consumption. Downstream of the compression, a simple separator model mimics the removal of excess oxygen and water, which would otherwise violate the specifications for liquid CO_2 transport adopted from the Northern Lights project [64]. The liquefaction process operates with an ammonia refrigeration cycle, as described by Deng et al. [63], similar to the refrigeration cycle considered in the carbon capture project at the waste-to-energy plant at Klemetsrud [65]. The specification of the outgoing liquid CO_2 stream was set to 16 bar and −26.5 °C, thereby resembling the specifications made in the Northern Lights project [64], which considered ship transport of CO_2 for permanent sub-seabed storage. Important assumptions regarding the process parameters of the CO_2 compression and liquefaction processes are listed in Supplementary Materials S.2. Finally, to evaluate the performances of the capture models, the following technology performance indicators were considered, as defined in Eqs. (1)–(5):

$$\text{HPC loading } (\alpha_{HPC}) = \frac{[HCO_3^-]}{[K^+]} \left[\frac{mol}{mol}\right] \tag{1}$$

$$\text{MEA loading } (\alpha_{MEA}) = \frac{x_{CO_2}}{x_{MEA}} \left[\frac{mol}{mol}\right] \tag{2}$$

$$\textit{Specific reboiler duty}(SRD) = \frac{Q_{reboiler}}{\dot{m}_{CO_2,captured}} \left[\frac{MJ}{kg_{CO_2}}\right] \tag{3}$$

$$\textit{Specific power demand} = \frac{Net\ power\ consumption}{\dot{m}_{CO_2,captured}} \left[\frac{MJ}{kg_{CO_2}}\right] \tag{4}$$

$$Specific\ cooling\ demand = \frac{Net\ cooling\ demand}{\dot{m}_{CO_2,captured}}\left[\frac{MJ}{kg_{CO_2}}\right] \qquad (5)$$

2.1.2. Bio-CHP plant steam cycle model

A steady-state model of the reference bio-CHP plant steam cycle was developed in EBSILON Professional based on available plant data and general CHP design principles. Fig. 3 presents a schematic of the main steam cycle components modeled. The boiler, which is modeled as a steam generator with a fixed efficiency of 92% based on [7], produces live steam at a pressure of 136 bar and temperature of 558 °C. The live steam is expanded in a steam turbine in six stages, where steam is extracted to feedwater preheaters, a deaerator, and two DH condensers. Input data are given for the turbine extraction pressures and DH target temperatures. The isentropic efficiency of the steam turbine is assumed to be 88%. Based on the given fuel input, the model calculates the electricity generation and DH generation of the steam cycle.

For the CHP-HPC plant, live steam is extracted to drive the flue gas compressor and to supply heat to the capture process (depicted with black dashed lines in Fig. 3). For the CHP-MEA plant, low-pressure steam for powering the capture process is extracted from the turbine at the deaerator stage. The steam condensate from the capture process is returned to the deaerator in both cases. The energy requirements of the capture process (reboiler duty and power demand of the flue gas compressor) are given as inputs based on the capture plant process modeling, as described in Section 2.1.1.

2.2. Plant and extended system boundaries and performance evaluation

2.2.1. CHP-CCS plant boundary

The reference bio-CHP plant model is assumed to be retrofitted with CO_2 capture, compression, and liquefaction units. Heat is recovered within the bio-CHP plant through wet-gas cleaning of the exhaust gases in a flue gas condenser and the turbine condenser. This is to provide heat to the DH supply water (depicted with solid red lines in Fig. 4). With the integration of the CCS unit, it is expected that additional excess heat can be recovered through condensation of the CO_2-rich stripper top gas, the

flue gas stream from the absorber top, the lean solvent cooler, and the heat of compression from the compression and liquefaction processes. The total heat recovered from these processes is shown in Fig. 4, denoted as $Q_{recovered}$, which, together with the heat recovered from the bio-CHP plant, is the total heat delivered by the CHP-CCS plant to the DH network, denoted as Q_{CHPCCS}.

Steam and electricity are internally consumed to drive the carbon capture process, compression, and liquefaction, denoted as Q_{CC} and P_{CC}, respectively. The net amount of electricity that is not used on-site is supplied to the grid, which is denoted as P_{CHPCCS}. Finally, the remaining output streams are the liquefied CO_2 stream at 20 °C, the DH water supply at 86 °C, and the CO_2-depleted flue gas cooled to 42.5 °C from the carbon capture plant. With this system boundary, the energy and exergy flows of the CHP-CCS plant are evaluated for the three cases listed in Table 3: CHP-MEA, CHP-HPC, and CHP-MEA-HP. Since the CHP-MEA plant is expected to consume less power than the CHP-HPC plant [13], the surplus power (net delivered electric power from case CHP-MEA minus that from CHP-HPC) can be used instead to drive a centralized heat pump so as to provide additional heat. This is done in the CHP-MEA-HP configuration, which is modeled following two constraints: (i) the net power output must be the same as for the CHP-HPC case, and (ii) it is assumed that the heat pump upgrades excess heat from temperatures lower than the DH return temperature of 47 °C to the DH supply temperature of 86 °C. Here, the lower temperature limit is set by the maximum temperature lift of 60 °C, which is assumed in the heat pump. This assumption results in the lowest possible temperature of 26 °C. Thus, unutilized waste heat in the temperature range of 26°–47 °C is considered to be available for upgrading to the DH supply temperatures using centralized large-scale heat pumps in the CHP-MEA-HP case. Therefore, the net delivered power to the grid in the CHP-MEA-HP case is equal to that of the CHP-HPC case.

The cases listed in Table 3 are evaluated for their energy performances using the CHP plant performance indicators defined in Eqs. (6)–(9).
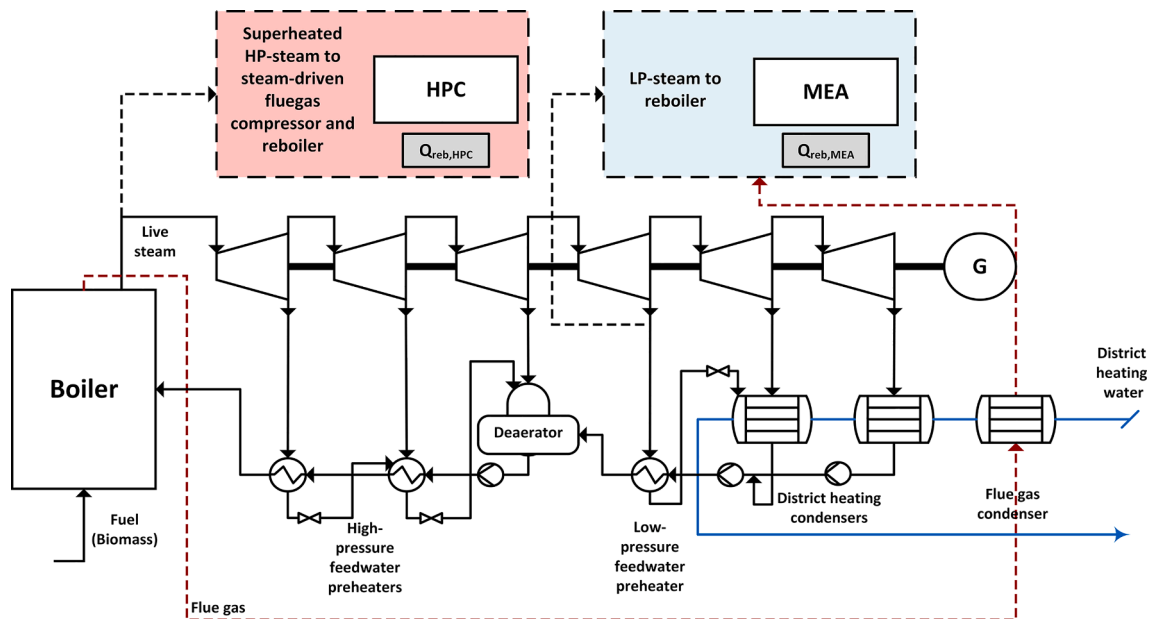

Fig. 3. Process schematic of the CHP steam cycle modeled for the reference plant, adapted from Beiron et al. [3]. Note that only one of the two CCS units is considered when evaluating the CHP-MEA or CHP-HPC case. Note also that the FGC (shown in Fig. 2) is now placed outside the CCS unit blocks to represent the CHP steam cycle more accurately. Black dashed lines – steam extracted from the steam cycle to drive the corresponding CCS unit; Red dashed lines – flue gases from the boiler; Gray boxes – input data to the CHP steam cycle model. (For interpretation of the references to colour in this figure legend, the reader is referred to the web version of this article.)
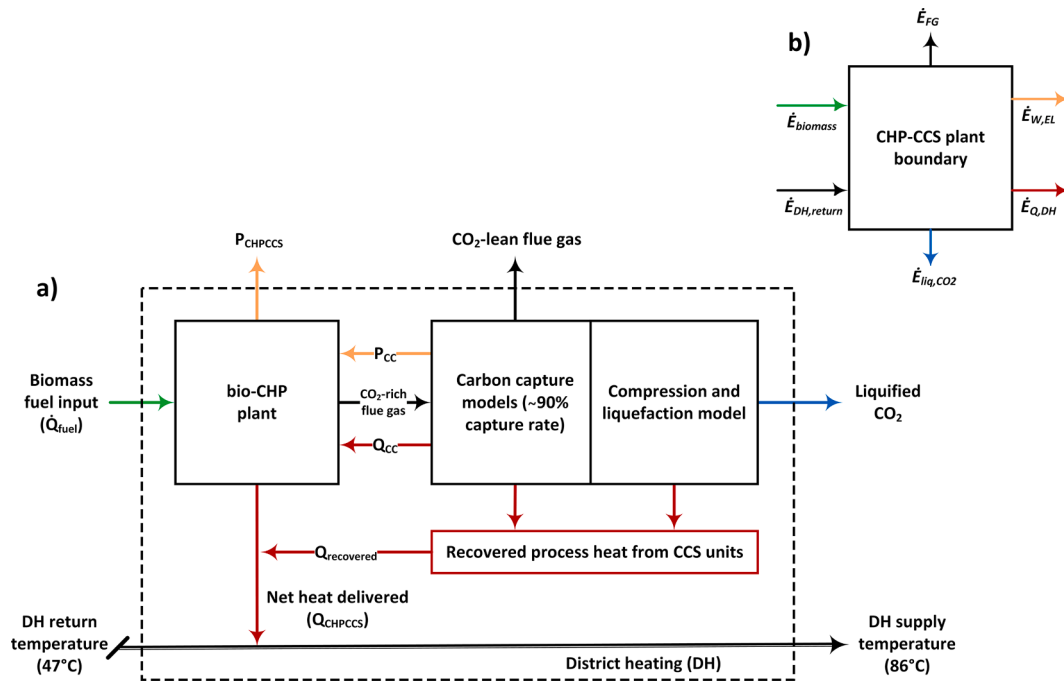
Fig. 4. Schematic of the CHP-CCS plant boundary. a) with the reference bio-CHP plant model integrated with carbon capture and CO_2 conditioning process models; and b) the exergy flows of the CHP-CCS plant boundary. Note that material streams, e.g., combustion air, makeup feedwater, and other makeup streams, are neglected.

Table 3
Cases investigated within the plant system boundary.

Case investigated	Description
CHP-MEA	CHP model integrated with the MEA model and CO_2 conditioning models
CHP-HPC	CHP model integrated with the HPC model and CO_2 conditioning models
CHP-MEA-HP	Heat pump integrated into the modeled CHP-MEA process – to balance the amount of net power delivered in the CHP-MEA case with that in the CHP-HPC case

$$\eta_{CHPCCS} = \frac{(P_{REF} - P_{CC}) + (Q_{REF} - Q_{CC}) + Q_{recovered}}{m_f \cdot HHV_{fuel}} \times 100 \ [\%] \quad [6]$$

$$\qquad\qquad (6)$$

$$= \frac{P_{CHPCC} + Q_{CHPCC} + Q_{recovered}}{\dot{Q}_{HHV_{fuel}}} \times 100 \ [\%] \quad [7]$$

$$Power\ preservation\ (CHP_{PP}) = \frac{P_{CHPCC}}{P_{REF}} \times 100 \ [\%] \quad (8)$$

$$CHP_{pen} = \frac{(P_{REF} + Q_{REF}) - (P_{CHPCC} + Q_{CHPCC} + Q_{recovered})}{(P_{REF} + Q_{REF})} \times 100 [\%] \quad (9)$$

The energy efficiency of the CHP-CCS plant (η_{CHPCCS}) is calculated as shown in Eq. (6), which represents the heat and electric power output from the plant in relation to the higher heating value of the fuel input (HHV_{fuel}). Here, the higher heating value (HHV_{fuel}) of fuel input is considered, since the heat of condensation of the fuel moisture is recovered as useful heat in the flue gas condenser at temperatures suitable for DH water. Q_{REF} and P_{REF} terms are the heat and power production, respectively, of the reference CHP plant operating without CO_2 capture. Q_{CC} and P_{CC} are the heat and power consumption, respectively, of the CO_2 capture and conditioning processes, and $Q_{recovered}$ is the low-temperature heat that is recoverable (via direct heat exchange and centralized large-scale heat pumps, if applicable) from these CCS units, as shown in Fig. 4. In the CHP-MEA-HP case, the

additional electric power consumed in the centralized large-scale heat pump is included in the total power consumption levels of the associated CO_2 capture process, denoted as P_{CC}. Equation (6) is further simplified, as shown in Eq. (7), as the ratio of the sum of the net heat (Q_{CHPCC}) and the net electric power production (P_{CHPCC}), and the recoverable heat ($Q_{recovered}$) to the fuel input ($Q_{HHV,fuel}$). Furthermore, power preservation (adapted from Gustafsson et al. [7]) is defined in Eq. (8) as the ratio of the retained (or preserved) electric power output by the CHP plant following the integration of the CCS units or the net electric power output (P_{CHPCC}) from CHP-CCS plant to the net electric power output (P_{REF}) of the reference CHP. Finally, the energy penalty (CHP_{pen}), as defined by Gustafsson et al. [7], is defined as the percentage change in the energy efficiency of the reference CHP plant following the integration of carbon capture processes.

The exergy performance of the three cases (Table 3) is compared within the bio-CHP plant system boundary. The exergetic efficiency is defined in Eq. (10) as the ratio of all exergy flows exiting the plant system boundary (denoted with the "-" sign) to all exergy flows entering the plant system boundary (denoted with the "+" sign), under atmospheric conditions (T_{ref} = 298.15 K and P_0 = 1.01325 bar) taken as the reference environment [66]. The specific exergy (e) of each material stream (i) is defined as the sum of the thermal exergy, kinetic and potential exergy related to a reference environment, where thermal exergies include both the physical and chemical exergies of a material stream [66]. The kinetic and potential exergies are neglected, as is typically done when evaluating stationary, steady-state processes. Work streams ($\dot{E}_W$) are considered to have pure exergy, i.e., the energy flow is equal to the exergy flow, whereas for heat flows, the exergy ($\dot{E}_q$) is calculated according to Eq. (11), in that it is related to the Carnot factor, where T_{ref} (K) is the reference temperature, and T (K) is the temperature at which heat is supplied or delivered to the system. In this case, the heat delivered as DH supply water is at 86 °C.

In Fig. 4b, all the associated exergy streams of the CHP-CCS plant boundary are shown, where the input exergy streams are the fuel input and DH return water, and the main output exergy streams comprise liquefied CO_2, CO_2-depleted gas, and the net power and heat delivered to the grid and DH network, respectively. Other material streams, such

as combustion air and makeup boiler feedwater, are neglected because they typically contribute significantly less to the total exergy input than the fuel exergy input. The Aspen Plus property set EXRGYFL is used to estimate the physical exergies of material streams, while the chemical exergies of the material streams are computed manually. For example, Eq. (12) is used for gaseous mixtures, such as a CO_2-depleted flue gas stream leaving the CHP-CCS plant. In Eq. (12), x_j is the mole fraction of the gas component in the gas mixture, and $e_{j,ch}^0$ is the standard chemical exergy of the gas component j in the mixture, relative to its reference environment [66]. In this work, wood chips (moisture content ~ 50%, $HHV_{as-received}$ ~ 10.1 MJ/kg or $LHV_{as-received}$ ~ 8.1 MJ/kg [7]) are assumed to be the primary fuel for the reference CHP plant. The standard chemical exergy of biomass is computed using the correlation factor proposed by Szargut et al. [66] for solid technical fuels, from which the exergy flow is estimated. A factor of 1.06 is estimated between the standard chemical exergy and the lower heating value (LHV) for the wood chips. Finally, the exergy efficiency of the CHP-CCS plant is calculated as per Eq. (13), which relates the system exergy output to the total exergy input to the defined CHP-CCS system boundary, as shown in Fig. 4a.

$$\eta_{ex} = \frac{\sum_i m_i^- \cdot e_i + \sum \dot{E}_w^- + \sum \dot{E}_q^-}{\sum_i m_i^+ \cdot e_i + \sum \dot{E}_w^+ + \sum \dot{E}_q^+} \quad (10)$$

$$\dot{E}_q = \left(1 - \frac{T_{ref}}{T}\right) \cdot \dot{Q} \quad (11)$$

$$e^{ch} = \sum_j x_j e_{j,ch}^0 + RT_{ref} \sum_j x_j ln(x_j) \quad (12)$$

$$\eta_{ex_{CHP-CCS}} = \frac{\dot{E}_{Q,DH} + \dot{E}_{W,el} + \dot{E}_{liq,CO_2} + \dot{E}_{CFG}}{\dot{E}_{biomass} + \dot{E}_{DH,return}} \quad (13)$$

2.2.2. Extended system boundary

Fig. 5a shows the extended system boundary with the local DH system. Note that the CHP-CCS plant boundary is within the extended system boundary, with the final energy service being end-use heat consumed in the local DH system. There are two components to the delivered heat: i) heat supplied as DH supply water, and ii) heat supplied by the decentralized GSHPs at the demand side, using the net electric power delivered to the electricity grid. Apart from the delivered heat,

the other main outputs from the extended system boundary are the cleaned flue gas stream and the liquefied CO_2 from the CHP-CCS plant.

Fig. 5b shows the input and output exergy flows for the extended system boundary, where the heat is consumed at an end-use temperature in the range of 30°–60 °C, thus incorporating the losses associated with decentralized GSHPs, conversion losses linked to the technical systems of the buildings, and DH and electric power transmission losses. A representative range for the coefficient of performance (COP) of the GSHPs was estimated (see Supplementary Materials S.3), assuming a constant heat source temperature of 10 °C and a Carnot efficiency in the range of 40–60%. While the heat source temperature is kept constant, the range of Carnot efficiency (40–60%) is chosen to represent any influence of external conditions, such as seasonal changes in ground temperatures, on the COP of the decentralized GSHPs The exergy efficiency of the CHP-CCS plant operating within its extended system boundary, denoted as $\eta_{ex,ext-sys}$, is defined in Eq. (14) as the ratio of the exergy outflows, i.e., the primary DH delivered ($\dot{E}_{Q,DH}$), end-use heat delivered by the GSHPs ($\dot{E}_{Q,GSHPs}$), liquefied CO_2 ($\dot{E}_{liq,CO_2}$), and the clean flue gas stream ($\dot{E}_{CFG}$), to the main exergy inflow, i.e., the DH return water and the biomass fuel input to the CHP-CCS plant. Note that the exergy flows of the combustion air, feedwater makeup, and other makeup streams are neglected, as they are expected to have lower input exergy flows (estimated to be < 1.5% for steam power plants [66]) in relation to the fuel exergy and DH return water in the CHP-CCS plant

$$\eta_{ex,ext-sys} = \frac{\dot{E}_{Q,DH} + \dot{E}_{Q,GSHPs} + \dot{E}_{liq,CO_2} + \dot{E}_{CFG}}{\dot{E}_{biomass} + \dot{E}_{DH,return}} \quad (14)$$

3. Results

3.1. Comparison of the technical performances of HPC-based and MEA-based CO_2 capture processes

The technology performance indicators for the two CO_2 capture technologies, capturing 90% CO_2 from a typical flue gas stream from a biomass-fired boiler with approximately 16 vol.% (wet basis) CO_2, are shown in Table 4. The grand composite curves (GCCs) of the MEA and HPC capture processes, including the compression and liquefaction units, are shown in Fig. 6. Utility targeting was performed to estimate the amounts of potentially recoverable excess heat in these units,
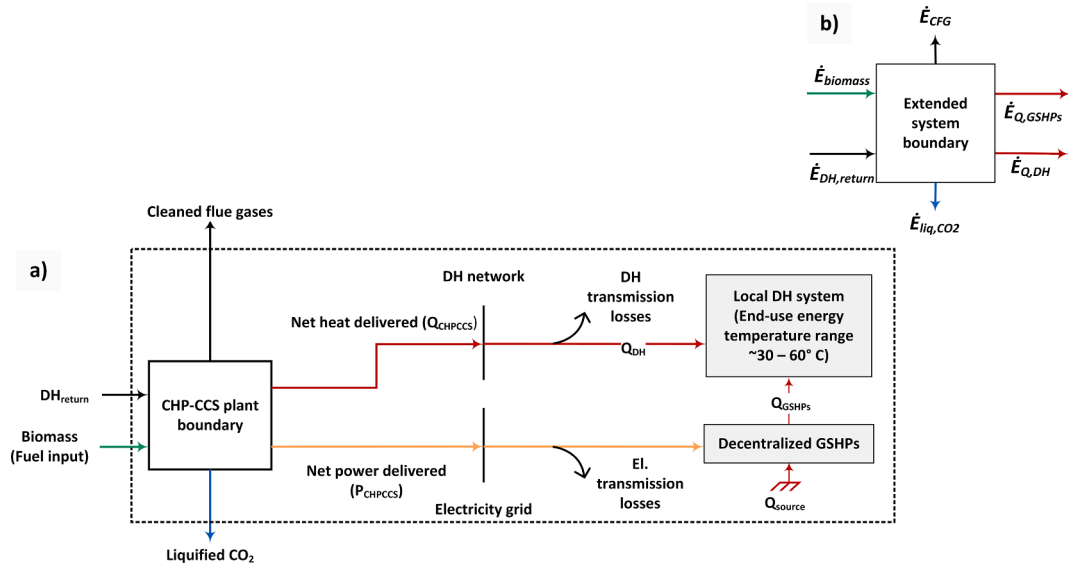

Fig. 5. A) extended system boundary with the energy service provider (chp-ccs plant) and the energy service consumers (local dh system), where it is assumed that the electric power generated is consumed entirely in decentralized ground source heat pumps (gshps), thereby maximizing the heat delivered to the system. b) the exergy flows of the extended system boundary.

Table 4

Comparison of the HPC and MEA processes for a capture rate of 90% with 16 vol. % CO_2 (approximately 130–132 tCO_2 captured per hour), which is representative of a wet flue gas stream from a biomass-fired boiler. Note that only the CO_2 capture sections are compared (excludes the compression and liquefaction units).

Technology performance indicators	Unit	HPC	MEA
CO_2 capture section			
Specific reboiler duty (SRD)	MJ/kgCO_2	3.44	3.67
Heat recovered from flue gas compression (42.5 °C–199 °C)	MJ/kgCO_2	1.09	–
Net hot utility requirement	MJ/kgCO_2	3.02	3.67
Specific cooling demand	MJ/kgCO_2	3.06	3.61
Specific power demand	MJ/kgCO_2	0.44	0.05
Reboiler temperature	°C	116.6	126.7
Lean loading	mol/mol	0.21	0.20
Rich loading	mol/mol	0.78	0.50
Solvent makeup	kg/tCO_2	45.77	584.26
Cyclic capacity	molCO_2/kg solvent	1.26	1.37
Liquid-to-gas ratio (absorber)	kg/kg	5.23	3.48
Solvent standard volumetric flow rate	m³/h	1586	1369
Specific packing volume (absorber and stripper)	m³/tCO_2/h	6.31	15.55
Specific heat exchanger area	m²/tCO_2/h	364.6	333.6
Total specific energy demand for CO_2 capture	MJ/kgCO_2	3.46	3.73
Including a CO_2 compression and liquefaction section (0.37 MJ/kgCO_2)			
Recoverable excess heat (47–86 °C) from CO_2 capture, compression, and liquefaction units	MJ/kgCO_2	0.99	0.58
Total specific power demand	MJ/kgCO_2	0.82	0.41
Total specific cooling demand	MJ/kgCO_2	4.74	4.27
Total specific energy (heat and power) demand for CO_2 capture, compression, and liquefaction	MJ/kgCO_2	3.84	4.09

primarily for DH delivery. Stream data for the GCCs are listed in the Supplementary Material (see Section S.2).

As expected, the SRD is lower for the HPC capture process than for the MEA process. Compared to the SRD, the net hot utility requirement (steam) remains unchanged for the MEA process, while it is reduced to 3.02 MJ/kgCO_2 for the HPC process when considering the recoverable excess heat from the capture plant alone. The net steam requirement is lower for the HPC process due to the heat that can be recovered from the intercooler of the two-stage flue gas compressor. The first stage of the compressor is driven by steam, whereas the second stage is driven by

expanding the pressurized cleaned flue gas that exits the top of the absorber. The recoverable excess heat in the flue gas intercoolers is approximately 1.09 MJ/kgCO_2 (42.5°–199 °C), a portion of which can be utilized for reducing the hot utility requirements (depicted with a solid red line in Fig. 6b). The reduction in the hot utility requirement, via heat recovery, for the HPC process is more than offset by its higher specific power demand, as compared with the MEA process, resulting in total specific energy demand for CO_2 capture that is only marginally lower for the HPC process (3.46 vs. 3.73 MJ/kgCO_2).

It is worth noting that the net hot utility demand accounts for 88% and 99% of the total specific energy demand for the HPC and MEA processes, respectively. Furthermore, the reboiler temperature in the HPC process is about 10 °C lower than in the MEA process, owing to the lower (optimal) stripper pressure. In addition, due to the higher absorber operating pressure in the HPC process, the specific packing (absorber and stripper) volume requirement is around 59% smaller, and the required solvent makeup is one order of magnitude lower (coupled with lower solvent volatility and water evaporation at higher pressures) than in the MEA process. However, the HPC process has a slightly lower cycling capacity and requires a 50% larger liquid flow in the absorber (on a mass basis), which increases the pressure drop across the packing (thereby increasing power consumption). The compression and liquefaction processes add 0.37 MJ/kgCO_2 in power demand to the CO_2 capture processes.

As shown in Fig. 6, the GCC of the HPC process is almost linear below the pinch point, as compared with the MEA process, which enables significantly higher levels of heat recovery for the DH network at the two defined levels, i.e., high-grade heat (61°–86 °C) and low-grade heat (46°–61 °C). Note that the amount of high-grade heat recovered for DH delivery is roughly 65% higher for the HPC process than for the MEA process. The heat recovery estimated for each CCS process in Fig. 6 is then used to estimate the CHP-CCS plant performance in the following section.

3.2. Performance of the CHP-CCS plant

3.2.1. CHP-CCS plant boundary

Fig. 7 shows the energy performances of the CHP-CCS cases (see Table 3) within their plant boundaries, as compared to the reference plant without CCS. The figure indicates significant differences between the two capture processes. For the MEA process, the energy required for
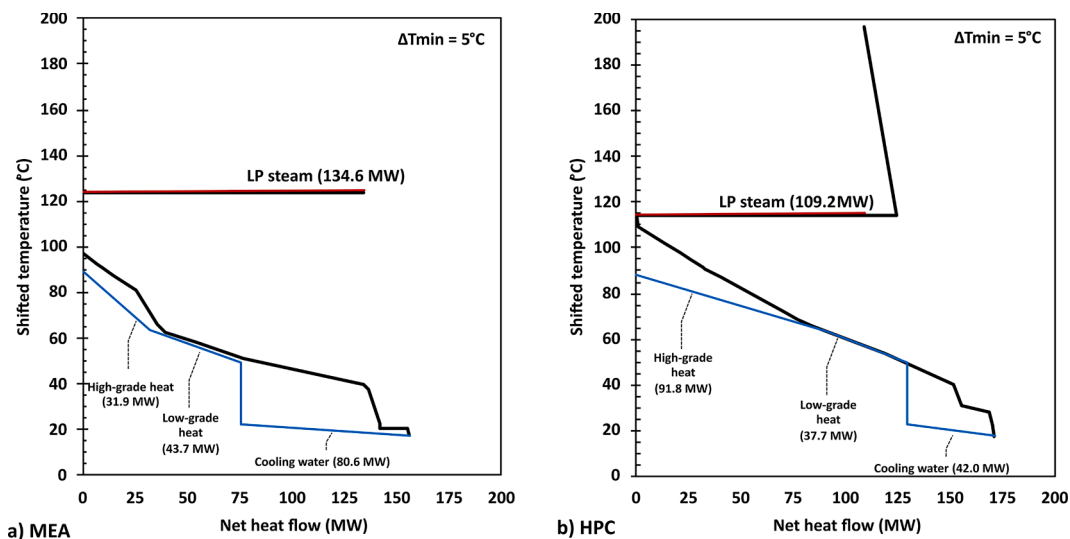
Fig. 6. Grand composite curves (with $\Delta T_{min} = 5$ °C) of the a) MEA process and b) HPC process, including the compression and liquefaction units. The solid blue line indicates the cold utility curve, indicating the three cold utilities, i.e., cooling water and high- and low-grade heat recovered for the DH water. The solid red line indicates the hot-utility curve (low-pressure steam) that is consumed at a slightly higher temperature in the MEA process (126.6 °C) than in the HPC process (116.6 °C). (For interpretation of the references to colour in this figure legend, the reader is referred to the web version of this article.)
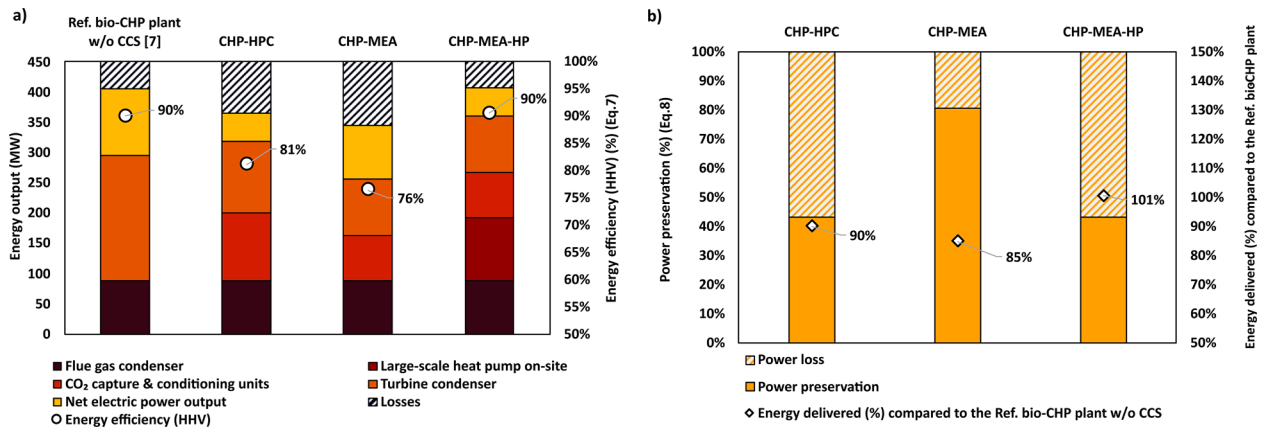
Fig. 7. A) net electric power outputs and shares of the net heat outputs from different heat recovery units in the chp-ccs cases, and the corresponding energy efficiencies (hhv) (eq.(7)) compared to the reference CHP plant without CCS units. b) Power preservation calculated as per Eq. (8), and energy delivered in the CHP-CCS cases compared to the reference bio-CHP plant.

the capture process corresponds primarily to the internal steam consumption level, resulting in a lower turbine condenser heat output than in the CHP-HPC case. Similarly, increased internal consumption of electric power for flue gas compression in the CHP-HPC case results in lower electric power output than in the CHP-MEA case. As a result, the total energy outputs for the CHP-MEA and CHP-HPC cases are similar, in the range of 345–366 MW, with different power-to-heat ratios in the two cases. Fig. 7a and Fig. 7b also show the energy efficiencies of the CHP-CCS cases and the energy penalties (as defined by Eq. (7)). The MEA case incurs the highest energy penalty (roughly ∼ 15%). Thus, the HPC process (with a significantly lower energy penalty) is more favorable for a bio-CHP plant that operates as a baseload unit in a DH system.

However, the higher levels of preserved power (roughly 80%, see Fig. 7b) in the CHP-MEA plant could be used internally to upgrade the low-grade heat (i.e., unutilized below the DH return temperature of 46 °C) to the desired DH supply temperature of 86 °C using a heat pump (CHP-MEA-HP). The heat pump COP was estimated at 2.54, considering that the unutilized low-grade heat (in the range of 26°–47 °C) is upgraded entirely using the preserved electric power in the CHP-MEA case. Furthermore, a heat pump with higher efficiency would result in a lower specific power demand to upgrade the same limited amount of unutilized low-grade heat, resulting in an increased total energy output from the CHP-CCS plant. Thus, the estimated COP is deemed to be rather conservative compared to similar heat pumps operating within CHP

plants, which have COPs in the range of 3.3–3.5 [27]. Therefore, integrating a heat pump (CHP-MEA-HP) results in a higher energy output than the CHP-HPC case and roughly the same energy output as the reference plant without CCS, as shown in Fig. 7a. The energy delivered compared to the reference bio-CHP plant (%), shown in Fig. 7b, could be alternatively presented as the energy penalty (as defined in Eq. (9)). Thus, the resulting energy penalty for the CHP-MEA-HP is approximately −1%, indicating a similar or slightly higher energy output compared with the reference CHP plant without CCS. The difference lies in the energy mix of the total energy output, where the total heat delivered is roughly 21% higher than in the reference CHP plant (and the electric power delivered is correspondingly lower). From the CHP plant operator's perspective, using the energy penalty as a figure of merit to compare different capture technologies, it is clear that the CO_2 capture technology (HPC process) that minimizes DH delivery losses is the preferred option.

In contrast, the electric power output retained by the MEA process in the CHP-MEA plant could be consumed on-site to increase DH delivery or delivered to the electricity grid. The choice between the two CO_2 capture technologies comes down to electricity consumption in heat pumps versus flue gas compressors in the HPC process, followed by heat recovery in the new CCS units. In any case, the CHP-MEA-HP would be the most-effective solution to maximize heat delivery to the DH system, as shown in Fig. 7. The exergy performances of the CHP-CCS cases
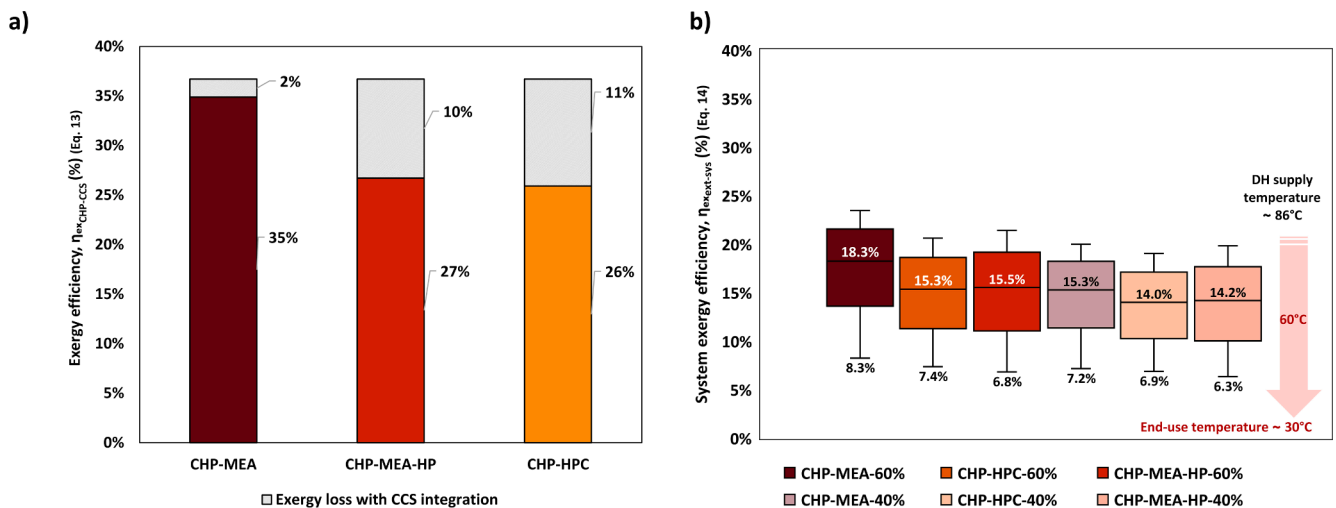

Fig. 8. Exergy efficiencies of the CHP-CCS plant cases within their plant boundaries a) and extended system boundaries b), with GSHPs operating with Carnot efficiencies η_{Carnot} in the range of 40%–60%.

within their plant boundaries are presented in the following section to highlight the differences that emerge when the system boundary is extended to the end-users of the delivered heat.

3.2.2. Extended system boundary

Fig. 8a shows the exergy performances of the CHP-CCS cases within their plant boundaries, where the CHP-MEA case has the highest exergy efficiency (approximately 35%), primarily due to its higher power preservation compared to the other two cases. It is important to note here that only a fraction of the preserved electric power output in the CHP-MEA case is consumed (see Fig. 7) to drive large-scale heat pumps on-site (CHP-MEA-HP case) to have the same exergy output as the CHP-HPC case (see Fig. 8a). As a result, the total DH output of the CHP-MEA-HP case is about 12% and 41% higher than CHP-HPC and CHP-MEA cases, respectively. This is an example of the product flexibility inherently offered to a BECCS plant with higher exergy efficiency. The bio-CHP plant fitted with the MEA process and large-scale heat pumps within their plant boundary has greater availability of higher-exergy energy carrier, electricity, that could be strategically used in heat pumps to increase the total DH output or delivered to the electricity grid. Here, product flexibility is defined as the ability of the bio-CHP plant to vary the output load of a specific product by adapting the product ratios, i.e., between heat, power, and negative CO_2 emissions. It is important to recall that this study adopts a conservative approach by evaluating the MEA capture technology with a 90% capture rate, which could, in reality, also have the possibility to capture beyond 90%, if required, with a marginal increase in specific capture costs. In addition, the benchmark amine solvent considered here incurs a much higher SRD (3.67 MJ/kg CO_2, see Table 4) at a 90% capture rate than state-of-the-art amine solvent blends (for example, the blend of 2-amino-2-methyl-1-propanol (AMP) and piperazine (PZ), incurred roughly 3.41–3.54 MJ/kgCO_2 at a capture rate of 97–99% [36]). However, a higher capture rate (>90%) is not an option applicable to the HPC process because significant amounts of exergy need to be expended to drive the flue gas compressors and operate the capture units at higher pressures.

Fig. 8b shows the exergy efficiencies of the three CHP-CCS cases estimated with the extended system boundary approach. The maximum values in the box plots indicate the exergy efficiencies estimated for a DH supply temperature of 86 °C. The minimum and median values represent the exergy efficiencies corresponding to typical end-use supply temperatures, in the range of 30°–60 °C for space heating and domestic hot water, respectively. Overall, the CHP-MEA case yields the highest exergy efficiency when heat is assumed to be delivered within the end-use supply temperature range. This result is expected due to the higher retained electric power output within the CHP-MEA plant boundary, resulting in higher end-use energy output in the extended system boundary. While the difference in exergy efficiency between CHP-HPC and CHP-MEA-HP cases is minimal, the total DH heat delivered at the DH supply temperature of 86 °C is roughly 12% higher in the CHP-MEA-HP cases with the centralized heat pump, as depicted by the maximum value in the box plots. Fig. 8b illustrates the expected system exergy efficiency range, with assumed Carnot efficiency (η_{Carnot}) in the range of 40–60% for the GSHPs.

At an end-use temperature of 60 °C, the system exergy efficiency is roughly 3 percentage points higher for the CHP-MEA plant than for the CHP-HPC and CHP-MEA-HP cases at 60% (η_{Carnot}). However, this difference in system exergy efficiency for the CHP-MEA plant diminishes to 1 percentage point at 40% (η_{Carnot}), indicating lower levels of end-use heat delivered. Nevertheless, the COP estimated for the upper bound of the end-use supply temperature of 60 °C is in the range of 2.7–4.0 (η_{Carnot} ~ 40–60%) (see Supplementary Materials S.3), which is reasonable for commercial GSHPs. Additional exergy efficiency plots are presented in Supplementary Materials S.4, for all the cases, within their plant boundaries, and with the extended system boundaries, with varying supply temperatures and Carnot efficiencies (η_{Carnot}). The system exergy efficiency is highest when the retained electric power output

is consumed locally in decentralized GSHPs (CHP-MEA), followed by the case where it is consumed on-site in centralized large-scale heat pumps (CHP-MEA-HP), and finally, the CHP-HPC case, which exhibits the lowest system exergy efficiency owing to its lower power-to-heat ratio. These results show that high levels of DH delivery can be achieved with the uptake of GSHPs into the local energy systems, which can use the retained electric power output in power-to-heat technologies to avoid DH distribution losses. Thus, further emphasizing that the CO_2 capture technology (MEA) that retains the electric power output of a bio-CHP plant is preferable to the HPC process. It is evident here that using exergy as a figure of merit leads to divergence in the optimal CHP-CCS plant configuration (indicated in Section 3.2.1) when viewed from both the CHP plant operator's (or investor's) perspective and the local DH system's perspective. In addition, consumers of end-use heating services in this local DH system could optimize their costs by connecting to the DH network or choosing competing domestic heat pump technologies. Alternatively, they could optimize their indoor climate demand patterns by complementing their existing heating systems with heat pumps.

4. Discussion

Bio-CHP plants operating in a DH system are considered highly suitable for extensive BECCS deployment to enable carbon dioxide removal from the atmosphere. However, in a DH system, the values allocated to the different energy services/carriers of an existing bio-CHP plant, i.e., heat and electricity, are different at the plant level than at the system level, which includes the consumers. This difference in value allocation is expected, as an energy carrier with higher exergy, i.e., electricity could be utilized for several different purposes (heating and cooling, but also any other power demands in households or industrial applications) in the local energy system. In contrast, from the bio-CHP plant operator's perspective, district heat delivery is prioritized over electricity power production due to the pre-existing local monopolies of CHPs in the Swedish DH system [30], while electric power is traded in the power market and is subject to competition and price volatility [27]. Thus, from the perspective of a bio-CHP plant operator in a DH system, the optimal carbon capture technology for large-scale BECCS implementation would be the technology that minimizes loss of heat sales. Therefore, several different options arise regarding how such a DH system could be optimized to implement BECCS efficiently and cost-effectively to meet national or regional climate goals.

4.1. Carbon capture processes

The rigorous numeric modeling of HPC and MEA capture processes reveals the inherent differences between the two processes when applied to the same flue gas stream with the same capture rate. The differences were quantified using the technology performance indicators listed in Table 4. These technology performance indicators could be used to estimate specific investment and operational costs per tonne of CO_2 captured from the two capture processes, which could be retrofitted to similar bio-CHP plants. The results indicate a marginally higher specific heat exchanger area requirement for the HPC process than the MEA process (due to a higher rate of solvent circulation), while smaller column volumes are required due to the higher operating pressures applied in the HPC process. Thus, it is recommended to quantify the spatial footprints of these two capture technologies when performing more-advanced feasibility studies.

Advanced process configurations, such as those involving absorber intercooling, rich-solvent splitting, and vapor compression, although not considered in this work, could reduce the specific energy requirements and, thereby, the operational costs of individual capture plants. In addition, the HPC process could operate at higher temperatures, i.e., the absorber and stripper could operate close to the solvent's boiling point, thereby reducing the SRD of the stripper. However, a high-temperature

configuration is typically suitable for industrial processes with high flue gas temperatures at the stack and no flue gas condensers in place, so it is deemed unsuitable for a CHP plant with flue gas condensers in place to maximize heat delivery to its DH system.

The MEA capture process modeled in this work is a conventional amine-based solvent with an estimated SRD of 3.67 MJ/kgCO$_2$, which is significantly higher than proprietary advanced amine solvents tested in recent years. For example, proprietary advanced amine solvents such as Shell Cansolv [67], Hitachi H3-1 [68], and MHI – KS1 [69] are reported to have specific heat demands in the range of 2.3–2.5 MJ/kgCO$_2$ for a typical capture rate of 90%. As mentioned previously, capture rates of up to 99% have been demonstrated with the CESAR-1 solvent, which is a blend of 2-amino-2-methyl-1-propanol (AMP) and piperazine (PZ), resulting in a specific heat demand in the range of 3.41–3.54 MJ/kgCO$_2$ [36]. The higher capture rates (~97–99%) achieved with the CESAR-1 solvent at a relatively similar range of specific energy demands as the benchmark MEA solvent highlights the development of amine-based capture processes. In contrast, the HPC process is very limited with respect to capture rates >90%, which would require significantly higher levels of energy being expended, in the form of heat and electricity, in the reboiler and the flue gas compressor to attain high operating pressures. The possibility to capture beyond 90% with advanced amine-based solvents, with minimal increase in operational costs, could be essential for a large-scale BECCS plant when accounting for the actual amount of CO$_2$ ultimately removed from the atmosphere over its extended cradle-to-grave system boundary that includes the impact of indirect land use change [70].

4.2. CHP-CCS plant boundary

At the plant level, the results presented in this work extend the work of Gustafsson et al. [7], who investigated retrofitting a bio-CHP plant for CO$_2$ capture using the HPC capture technology. Additional aspects considered in this work include: i) a comparison of the performance of the HPC process with that of an amine-based (MEA) capture technology; ii) an evaluation of the integration of heat pumps to upgrade low-grade heat that is rejected from the capture process. A comparison of the energy penalties for the two capture processes at the plant level indicates a higher penalty for the MEA process (~24%) than for the HPC process (~19%). However, the results presented in Section 3.2 indicate that the choice of capture technology is likely to be sub-optimal if the capture technology is chosen based on energy efficiency, as defined in Eq. (7), within the plant system boundary. Although it is clear that the HPC process has higher levels of available excess heat in the CO$_2$ capture and conditioning units compared to the MEA process, the higher power output (with low-carbon intensity) of the plant equipped with an MEA process could be exploited within the plant boundary to drive heat pumps, which would ultimately deliver more heat to the DH system. For example, within the plant boundary, the CHP-MEA-HP case with an on-site heat pump delivers more heat to the DH system than the CHP-HPC case while having the same electric power output to the electricity grid. These conclusions are not in accordance with the case made for the HPC capture process within plant boundaries by Gustafsson et al. [7] and highlight the limitations of the isolated comparisons presented in the literature for different carbon capture technologies applied to CHP processes that operate in a different context concerning their local energy system.

It should also be noted that the reference bio-CHP plant in Stockholm is an exception in relation to other bio-CHP plants operating in many DH systems in Sweden since it is a very large-scale CHP plant that delivers roughly 588 GWh of electricity and 1,468 GWh of heat to its local DH system annually, with roughly 6,000 full-load hours [71]. Thus, compared to other smaller bio-CHP plants in the region, this reference CHP plant, with large CO$_2$ flows (approximately 800 ktCO$_2$/yr) and a higher number of full-load hours, is expected to incur relatively lower specific capital costs for the capture plant [3]. In addition, the effect of

seasonal variations in electricity and DH demands is expected to play a significant role in minimizing the specific carbon capture costs. For example, a recent study carried out by Eliasson et al. [25] has reported comparable specific capture costs (in €/tCO$_2$) for a capture plant with seasonally varying (partial) capture rate that utilizes excess heat alone while maintaining the DH supply and for a capture plant that operates at constant load (full capture) at the expense of the DH supply. Thus, the design and operation (utilization hours, capture rate) are expected to confer further flexibility when the CO$_2$ capture plant is operated, depending on varying heating, cooling, and low-carbon electricity demands, as well as the scale of the reference plant. Aspects mentioned above, such as the operational flexibility of a CHP-CCS plant in relation to its local DH system, with seasonal variations in heat loads and temperatures, were outside the scope of this work. However, it is expected that the overall conclusion of this work will be unaffected, owing to the various possibilities that inherently come with the availability of high-exergy energy-carrier, i.e., electricity, in a BECCS plant with higher preservation of electric power production capacity.

Comparing the cases (see Table 3) investigated in this work, it is clear that the CHP-MEA-HP plant could achieve a higher level of heat delivery by including a heat pump, which could alternatively switch to a higher power output by shutting down heat pumps, depending on fluctuations in the heating and cooling demands over the year. Thus, the CHP-CCS plant could be operated as either a net-electric power exporter or importer depending on high or low electricity price periods, as previously discussed by Levihn [27]. Furthermore, higher operational and product flexibility, as defined by Beiron et al. [72], is expected for the CHP-MEA-HP plant. For example, the higher level of preserved electric power output in the CHP-MEA plant could be utilized optimally with heat pumps to meet the peak DH demand during winter months, and this could partially reduce dependence on heat-only boilers and, alternatively, provide low-carbon electricity, district cooling, and CO$_2$ removal, as services during the summer months. An analysis to identify a cost-optimal capture solution that minimizes specific CO$_2$ removal costs and maximizes profit with corresponding operational strategies for the CHP-CCS plant cases (see Table 3) was outside the scope of this work. Future work could focus on cost-optimization of operational and product (heat, power, and negative-CO$_2$ emissions) flexibility measures available to a future BECCS plant. Cost-optimization based on these aspects could be valuable to the future BECCS plant operator, as the proposed state aid for BECCS via the reverse auctioning system [73] in Sweden would be awarded to an industry or a bio-CHP plant that incurs the lowest costs.

4.3. Extended system boundary

Several factors in the extended system boundary could influence the optimal choice of carbon capture technology for the CHP-CCS, as compared to the rational choice of adopting the plant boundary. One of the external factors explored in this work is the performance of GSHPs that are operating within the extended system boundary. The results indicate a diminishing gap between the exergy efficiency of the CHP-MEA case with higher power preservation (80.6%) and its counterpart cases (CHP-HPC and CHP-MEA-HP) with lower power preservation (43.2%), as shown in Fig. 7b, with decreasing COP values for the GSHPs in the extended system boundary. In general, this means that, compared to a reference plant that would typically incur DH transmission losses in the DH network, with this hypothetical extended system boundary, the losses would occur locally in the GSHPs, in the form of conversion losses. Nevertheless, the lower-bound COP values estimated in this work (range of 2.7–4.0, for η_{Carnot} of 40–60%) are fairly conservative compared to the COPs reported for commercial GSHPs, which are in the range of 3.1–3.8 for a temperature difference of 50 °C [74]. Therefore, the inference made above holds for the extended system boundary defined in this work (see Section 2.2.2). Alternatively, if the delivered electric power is consumed elsewhere for an energy consumption end-use other than indoor space heating, the exergy efficiency of the overall system would

always be higher for the case with the highest power preservation, i.e., the CHP-MEA plant. Furthermore, from a Swedish perspective, electricity consumers are subject to considerably higher energy taxes than those levied on the power producers, who use the power themselves. Thus, providing further incentives to opt for a BECCS plant that operates with an MEA capture unit, complemented with a large-scale heat pump on-site to recover excess heat. This configuration could then be operated optimally based on the seasonal variations in the heat and power demands of the local DH system.

In the extended system boundary strategy, the uptake of GSHPs is also expected to face technical and regulatory challenges owing to the risk of net cooling of the ground in urban areas, as argued by Åberg et al. [32], whereby the regulations regarding distances between wells in urban areas are identified as critical for the potential competition between GSHPs and DH. Nevertheless, despite the current regulations on distances between wells, zones with competition between GSHPs and DH still exist in urban areas, such as Stockholm. In addition, the heat demand density (HDD), or the ratio of the buildings' DH demand to the land area that the buildings cover (kWh/m^2), could determine which CO_2 capture technology is optimal or, instead, which energy service should be prioritized in a future BECCS plant. For example, CHP plants operating in sparsely built areas yield a larger competitive region for GSHPs, as defined by Åberg et al. [32], and therefore have considerable incentive to preserve exergy with an MEA process, as compared to CHP plants operating in densely built areas with high HDD, where there is limited access to heat sources for GSHPs. In densely built areas, within regions in which there is competition with DH, other heat pumps such as air-source and ventilation or exhaust air heat pumps could be alternative solutions to meeting end-use heating needs with the preserved electric power output from the CHP-MEA plant. Another aspect that could be crucial in deciding on the optimal capture technology for a bio-CHP plant in the extended system boundary strategy, from the consumer's perspective, is the environmental risk associated with the capture solvent used. A comparative lifecycle assessment between MEA and potassium carbonate solvent [41] has indicated the significantly superior performance of the potassium carbonate solution for all environmental indicators considered in the study, including global warming, water use, ecotoxicity, and carcinogenic emissions.

5. Conclusions

This study compared the performance of two well-established but inherently different carbon capture processes (the hot potassium carbonate (HPC) process and the amine-based (MEA) process) for the capture of 90% of the biogenic CO_2 emissions from a typical flue gas stream of a bio-CHP plant in a DH system that mainly operates to provide heat as its primary energy service. In this context, a future transformation to a BECCS plant that additionally provides carbon dioxide removal (CDR) as a societal climate service will require careful selection of the carbon capture technology that minimizes the costs associated with implementing BECCS, for both the energy service provider and the consumers of this energy service.

A detailed process model of a large-scale bio-CHP plant in a DH system was developed and integrated with rigorous, rate-based carbon capture process models for the two capture processes, including the CO_2 compression and liquefaction train. The energy and exergy performance of the respective BECCS plants were evaluated within the plant boundary as well as its extended system boundary, considering that the delivered heat and power are used to meet the end-use heating needs in the local DH system. In addition, the integration of a centralized heat pump at the BECCS plant site to recover low-temperature heat from the BECCS plant was compared with a decentralized heat pump setting, using ground heat as the heat source. This was based on the possibility that the energy consumer might opt for increasing electricity usage to meet their indoor-climate needs, such as space heating and domestic hot water. Considering the same level of negative-emissions capacity (at

90% capture rate) from the two capture technologies, the results of this work indicate the following:

- From an energy perspective, for a bio-CHP plant, the MEA capture process incurs an energy penalty (defined as the change in the total energy efficiency of a CHP plant, considering heat and electric power output, resulting from the integration of CO_2 capture processes) of 15%–16%, which can be attributed to the low-temperature steam required to provide the heat need of the reboiler in the capture plantr, which in turn reduces the total heat output of the BECCS plant. In contrast, the HPC process results in an energy penalty of 9%–10%, albeit with significant electricity consumption in the flue gas compressors prior to the capture process.
- The MEA process has a higher level of power preservation (defined as the ratio of the electric power production capacity of a CHP plant with CCS to that of the same plant without CCS) than the HPC process. Thus, introducing an on-site heat pump to recover low-temperature heat with a conservative COP (~2.5) using the preserved power will lead to a significantly higher heat output (~12%). The corresponding energy penalty is −0.6%, indicating that the heat output is larger than that of the existing bio-CHP plant without the CCS units.
- The exergy efficiency of the bio-CHP plant is around 23% higher in the MEA process (~35%) than in the HPC process (~26%) due to the higher level of power preservation in the former within the plant system boundary. The same trends are observed when adopting the extended system boundary perspective for the BECCS plant with a decentralized DH system, considering the use of GSHPs in the local DH system to maximize the amount of heat delivered to the system. In this context, the difference in the exergy efficiencies of the two carbon capture technologies depends on how efficiently the GSHPs operate. Assuming a Carnot efficiency of 60% and a desired end-use target temperature in the range of 30°–60 °C (estimated COP ~ 4.0 at 60 °C), the MEA process would have a 10%–15% higher exergy efficiency than the HPC process, which would decrease to 4%–8% if a conservative Carnot efficiency of 40% (COP ~ 2.7 at 60 °C) were to be assumed.

According to these results, the MEA capture process clearly demonstrates a significant advantage over the HPC process for enabling BECCS, as it inherently offers greater product flexibility (i.e., the ability of the plant to vary a specific product output) with higher preservation of the electric power production capacity. Although a conservative approach with benchmark amine solvent was taken in this work, recent studies with advanced amine solvents have demonstrated that these solvents can also provide an opportunity to have capture rates up to 99% with minimal increase in specific energy demand, unlike the HPC process that reaches a techno-economic threshold at a capture rate of 90%. In addition, these state-of-the-art amine-based solvents have relatively lower environmental impacts than the benchmark MEA solvent. Considering energy performance as the primary figure of merit for different carbon capture technologies for a future BECCS plant could lead to sub-optimization of the societal services of a bio-CHP plant, incurring a higher economic cost for CDR as a service to Society. However, the optimal choice of carbon capture technology for a bio-CHP plant in a DH system will also depend on factors other than those considered here, such as techno-economics, the DH network density, seasonal variation in DH and power demands, and safety factors such as ecotoxicity, as well as other environmental repercussions of the capture solvents used in these carbon capture technologies.

CRediT authorship contribution statement

Tharun Roshan Kumar: Conceptualization, Methodology, Software, Data curation, Visualization, Validation, Writing – original draft. **Johanna Beiron:** Methodology, Software, Visualization, Validation,

Writing – original draft, Writing – review & editing. **Maximilian Biermann:** Methodology, Software, Visualization, Validation, Writing – original draft, Writing – review & editing. **Simon Harvey:** Funding acquisition, Project administration, Supervision, Writing – review & editing. **Henrik Thunman:** Conceptualization, Methodology, Funding acquisition, Supervision, Writing – review & editing.

Declaration of Competing Interest

The authors declare that they have no known competing financial interests or personal relationships that could have appeared to influence the work reported in this paper.

Data availability

Data will be made available on request.

Acknowledgment

Appendix A. Supplementary data

S.1 Hot potassium carbonate model–reactions list and model validation. S.2 CO_2 compression and liquefaction processes. S.3 Estimation of the coefficients of performance of heat pumps. S.4 Comparison of exergetic performances of the CHP-CCS cases. Supplementary data to this article can be found online at https://doi.org/10.1016/j.apenergy.2023.120927.

References

[1] Shukla PR, Skea J, Slade R, Khourdajie A Al, van Diemen R, McCollum D. IPCC, 2022: Climate Change 2022: Mitigation of Climate Change. Contribution of Working Group III to the Sixth Assessment Report of the Intergovernmental Panel on Climate Change. Cambridge University Press, Cambridge, UK and New York, NY, USA.; 2022. 10.1017/9781009157926.

[2] Ministry of the Environment and Energy. The Swedish Climate Policy Framework 2020:1–5. https://doi.org/10.5040/9781509941742.ch-007.

[3] Beiron J, Normann F, Johnsson F. A techno-economic assessment of CO_2 capture in biomass and waste-fired combined heat and power plants – A Swedish case study. Int J Greenh Gas Control 2022;118:103684. https://doi.org/10.1016/j.ijggc.2022.103684.

[4] Fuss S, Johnsson F. The BECCS Implementation Gap – A Swedish Case Study. Front Energy Res 2021;8:385. https://doi.org/10.3389/fenrg.2020.553400.

[5] IEA Bioenergy. Large biomass CHP plant in Stockholm Sweden 2018. https://www.ieabioenergy.com/wp-content/uploads/2018/02/8-LargeCHP-Värtaverket_SE_Final.pdf (accessed June 22, 2022).

[6] Stockholm Exergi's project for negative emissions receives EU support - Stockholm Exergi n.d. https://www.stockholmexergi.se/blogg/news-stockholmexergi/stockholm-exergis-project-for-negative-emissions-receives-eu-support/ (accessed June 22, 2022).

[7] Gustafsson K, Sadegh-Vaziri R, Grönkvist S, Levihn F, Sundberg C. BECCS with combined heat and power: assessing the energy penalty. Int J Greenh Gas Control 2021;110:103434. https://doi.org/10.1016/j.ijggc.2021.103434.

[8] Gadd H, Werner S. Achieving low return temperatures from district heating substations. Appl Energy 2014;136:59–67. https://doi.org/10.1016/J.APENERGY.2014.09.022.

[9] Kohl AL, Nielsen R. Gas Purification, Elsevier. Science 1997. https://doi.org/10.1016/B978-0-88415-220-0.X5000-9.

[10] Giammarco-Vetrocoke 2022. http://www.giammarco-vetrocoke.com/aboutus_history.htm (accessed October 24, 2022).

[11] CO2CAPSOL 2022. https://www.co2capsol.com/ (accessed October 24, 2022).

[12] Carbon Capture CCUs - CATACARB 2022. https://catacarb.com/applications/carbon-capture-ccus/ (accessed October 24, 2022).

[13] Levihn F, Linde L, Gustafsson K, Dahlen E. Introducing BECCS through HPC to the research agenda: The case of combined heat and power in Stockholm. Energy Rep 2019;5:1381–9. https://doi.org/10.1016/J.EGYR.2019.09.018.

[14] Djurberg R. Practical implementation of Bio-CCS in Uppsala: a techno-economic assessment, M.Sc. Thesis. Royal Institute of Technology, Stockholm, 2020. http://urn.kb.se/resolve?urn=urn:nbn:se:kth:diva-277820.

[15] Hammar C. Heat integration between CO_2 Capture and Liquefaction and a CHP Plant Impact on Electricity and District Heating Delivery at Renova's CHP Plant in Sävenäs, M.Sc. Thesis, Chalmers University of Technology, Gothenburg 2022. https://hdl.handle.net/20.500.12380/304511 (accessed June 22, 2022).

[16] Jilvero H. Ammonia as an Absorbent of Carbon Dioxide in Post-Combustion Capture-an Experimental, Technical and Economic Process Evaluation, Doctoral Thesis 2014. https://research.chalmers.se/en/publication/201381.

[17] Augustsson O, Baburao B, Dube S, Bedell S, Strunz P, Balfe M, et al. Chilled Ammonia Process Scale-up and Lessons Learned. Energy Procedia 2017;114:5593–615. https://doi.org/10.1016/j.egypro.2017.03.1699.

[18] Gardarsdóttir SÓ, Normann F, Andersson K, Johnsson F. Postcombustion CO_2 capture using monoethanolamine and ammonia solvents: The influence of CO_2 concentration on technical performance. Ind Eng Chem Res 2015;54:681–90.

[19] Jilvero H, Normann F, Andersson K, Johnsson F. Heat requirement for regeneration of aqueous ammonia in post-combustion carbon dioxide capture. Int J Greenh Gas Control 2012;11:181–7. https://doi.org/10.1016/j.ijggc.2012.08.005.

[20] Jilvero H, Normann F, Andersson K, Johnsson F. Thermal integration and modelling of the chilled ammonia process. Energy Procedia 2011;4:1713–20. https://doi.org/10.1016/j.egypro.2011.02.045.

[21] Jilvero H, Normann F, Andersson K, Johnsson F. Ammonia-based post combustion – The techno-economics of controlling ammonia emissions. Int J Greenh Gas Control 2015;37:441–50. https://doi.org/10.1016/J.IJGGC.2015.03.039.

[22] Pröll T, Zerobin F. Biomass-based negative emission technology options with combined heat and power generation. Mitig Adapt Strateg Glob Chang 2019;24:1307–24. https://doi.org/10.1016/B978-0-88415-220-0.X5000-9.

[23] Kärki J, Tsupari E, Arasto A. CCS feasibility improvement in industrial and municipal applications by heat utilization. Energy Procedia 2013;37:2611–21. https://doi.org/10.1016/j.egypro.2013.06.145.

[24] Eliasson Å, Fahrman E, Biermann M, Normann F, Harvey S. Integration of industrial CO_2 capture with district heating networks: a refinery case study. TCCS-11 2021:197–201. https://www.sintef.no/globalassets/project/tccs-11/tccs-11/sproceedings-no-7.pdf (accessed January 16, 2023).

[25] Eliasson Å, Fahrman E, Biermann M, Normann F, Harvey S. Efficient heat integration of industrial CO_2 capture and district heating supply. Int J Greenh Gas Control 2022;118:103689. https://doi.org/10.1016/j.ijggc.2022.103689.

[26] Abrami G. Energy targeting for heat recovery from carbon capture processes using hybrid absorption heat pumps, M.Sc. Thesis, Politecnico Di Milano, Milan, 2022. http://hdl.handle.net/10589/187439 (accessed July 8, 2022).

[27] Levihn F. CHP and heat pumps to balance renewable power production: Lessons from the district heating network in Stockholm. Energy 2017;137:670–8. https://doi.org/10.1016/J.ENERGY.2017.01.118.

[28] Beiron J, Göransson L, Normann F, Johnsson F. Flexibility provision by combined heat and power plants – An evaluation of benefits from a plant and system perspective. Energy Convers Manag X 2022;16:100318. https://doi.org/10.1016/J.ECMX.2022.100318.

[29] Beiron J. Combined heat and power plants in decarbonized energy systems, Doctoral Thesis. Chalmers University of Technology, Gothenburg 2022. https://research.chalmers.se/en/publication/531778.

[30] Werner S. District heating and cooling in Sweden. Energy 2017;126:419–29. https://doi.org/10.1016/j.energy.2017.03.052.

[31] Egüez A. District heating network ownership and prices: The case of an unregulated natural monopoly. Util Policy 2021;72:101252. https://doi.org/10.1016/J.JUP.2021.101252.

[32] Åberg M, Fälting L, Lingfors D, Nilsson AM, Forssell A. Do ground source heat pumps challenge the dominant position of district heating in the Swedish heating market? 2020;254. 10.1016/j.jclepro.2020.120070.

[33] Swedish Energy Agency. Värmepumparnas roll på uppvärmningsmarknaden - Utveckling och konkurrens i ett föränderligt energisystem (Heat pumps' role in the heat market - Development and competition in a changing energy market) 2015.

[34] Skatteverket. Energy tax on electricity n.d. https://www.skatteverket.se/foretag/skatterochavdrag/punktskatter/energiskatter/skattpael.4.15532c7b1442f256bae5e4c.html (accessed September 6, 2022).

[35] Biermann M. Partial CO_2 capture to facilitate cost-efficient deployment of carbon capture and storage in process industries, Doctoral Thesis. Chalmers University of Technology, Gothenburg 2022. https://research.chalmers.se/en/publication/531680.

[36] Hume S, Shah MI, Lombardo G, Kleppe ER. Results from CESAR-1 testing with combined heat and power (CHP) flue gas at the CO2 Technology Centre Mongstad. TCCS-11 2021:355–61.

[37] Brandl P, Bui M, Hallett JP, Mac DN. Beyond 90% capture: Possible, but at what cost? Int J Greenh Gas. Control 2021;105. https://doi.org/10.1016/j.ijggc.2020.103239.

[38] Danaci D, Bui M, Petit C, MacDowell N. En Route to Zero Emissions for Power and Industry with Amine-Based Post-combustion Capture. Environ Sci Technol 2021:55. https://doi.org/10.1021/acs.est.0c07261.

[39] Feron P, Cousins A, Jiang K, Zhai R, Shwe Hla S, Thiruvenkatachari R, et al. Towards Zero Emissions from Fossil Fuel Power Stations. Int J Greenh Gas Control 2019;87:188–202. https://doi.org/10.1016/j.ijggc.2019.05.018.

[40] Pérez-Calvo JF, Sutter D, Gazzani M, Mazzotti M. Pilot tests and rate-based modelling of CO2 capture in cement plants using an aqueous ammonia solution. Chem Eng Trans 2018;69:145–50. https://doi.org/10.3303/CET1869025.

[41] Grant T, Anderson C, Hooper B. Comparative life cycle assessment of potassium carbonate and monoethanolamine solvents for CO_2 capture from post combustion

flue gases. Int J Greenh Gas Control 2014;28:35–44. https://doi.org/10.1016/J.IJGGC.2014.06.020.

[42] Matin NS, Flanagan WP. Life cycle assessment of amine-based versus ammonia-based post combustion CO2 capture in coal-fired power plants. Int J Greenh Gas Control 2022;113:103535. https://doi.org/10.1016/j.ijggc.2021.103535.

[43] Gustafsson K. "Spearheading negative emissions in Stockholm's multi-energy system," Bioenergy with carbon capture and storage. From global potentials to domestic realities. Eur Lib Forum 2017;69–87. 10.1016/b978-0-12-805423-9.00004-1.

[44] Kemp IC. Pinch Analysis and Process Integration: A User Guide on Process Integration for the Efficient Use of. Energy 2019. https://doi.org/10.1016/B978-075068260-2.50007-9.

[45] Nikitin A, Deymi-Dashtebayaz M, Muraveinikov S, Nikitina V, Nazeri R, Farahnak M. Comparative study of air source and ground source heat pumps in 10 coldest Russian cities based on energy-exergy-economic-environmental analysis. J Clean Prod 2021;321:128979. https://doi.org/10.1016/J.JCLEPRO.2021.128979.

[46] Bravo JL, Rocha JA, Fair JR. Mass Transfer in Gauze Packings. Hydrocarb Process 1985;64:91–5.

[47] Stichlmair J, Bravo JL, Fair JR. General model for prediction of pressure drop and capacity of countercurrent gas/liquid packed columns. Gas Sep Purif 1989;3:19–28. https://doi.org/10.1016/0950-4214(89)80016-7.

[48] Chilton TH, Colburn AP. Mass transfer (absorption) coefficients prediction from data on heat transfer and fluid friction. Ind Eng Chem 1934;26:1183–7.

[49] Biermann M, Normann F, Johnsson F, Hoballah R, Onarheim K. Capture of CO2 from Steam Reformer Flue Gases Using Monoethanolamine: Pilot Plant Validation and Process Design for Partial Capture. Ind Eng Chem Res 2022;61:14305–23. https://doi.org/10.1021/acs.iecr.2c02205.

[50] Biermann M, Normann F, Johnsson F, Skagestad R. Partial Carbon Capture by Absorption Cycle for Reduced Specific Capture Cost. Ind Eng Chem Res 2018;57:15411–22.

[51] AspenTech. ENRTL-RK Rate-Based Model of the CO_2 Capture Process by MEA using Aspen Plus - Version 10.0. 2017.

[52] Notz R, Mangalapally HP, Hasse H. Post combustion CO_2 capture by reactive absorption: Pilot plant description and results of systematic studies with MEA. Int J Greenh Gas Control 2012;6:84–112. https://doi.org/10.1016/J.IJGGC.2011.11.004.

[53] Biermann M, Harvey S, Kjärstad Rahul Anantharaman J, Fu C, Jordal K, Reyes Lúa A, et al. Preem CCS Synthesis of main project findings and insights 2022. https://research.chalmers.se/en/publication/528685 (accessed January 16, 2023).

[54] Zhang Y, Chen CC. Modeling CO_2 Absorption and Desorption by Aqueous Monoethanolamine Solution with Aspen Rate-based Model. Energy Procedia 2013;37:1584–96. https://doi.org/10.1016/J.EGYPRO.2013.06.034.

[55] Pinsent BRW, Pearson L, Roughton FJW. The kinetics of combination of carbon dioxide with hydroxide ions. Trans Faraday Soc 1956;52:1512–20. https://doi.org/10.1039/tf9565201512.

[56] Hikita H, Asai S, Ishikawa H, Honda M. The kinetics of reactions of carbon dioxide with monoethanolamine, diethanolamine and triethanolamine by a rapid mixing

method. Chem Eng J 1977;13:7–12. https://doi.org/10.1016/0300-9467(77)80002-6.

[57] Kohl AL, Nielsen RB. Alkaline Salt Solutions for Acid Gas Removal. Gas Purification 1997. https://doi.org/10.1016/b978-088415220-0/50005-7.

[58] Berrouk AS, Ochieng R. Improved performance of the natural-gas-sweetening Benfield-HiPure process using process simulation. Fuel Process Technol 2014;127:20–5. https://doi.org/10.1016/j.fuproc.2014.06.012.

[59] Technology A. Physical Property Methods and Models 2011;11(1):1–19.

[60] Ayittey FK, Obek CA, Saptoro A, Perumal K, Wong MK. Process modifications for a hot potassium carbonate-based CO_2 capture system: a comparative study. Greenh Gases Sci Technol 2020;10:130–46. https://doi.org/10.1002/GHG.1953.

[61] AspenTech. ELECNRTL Rate-Based Model of the CO_2 Capture Process by K_2CO_3 using Aspen Plus - Version 12.1. n.d.

[62] Wu Y, Wu F, Hu G, Mirza NR, Stevens GW, Mumford KA. Modelling of a post-combustion carbon dioxide capture absorber using potassium carbonate solvent in Aspen Custom Modeller. Chinese J Chem Eng 2018;26:2327–36. https://doi.org/10.1016/J.CJCHE.2018.06.005.

[63] Deng H, Roussanaly S, Skaugen G. Techno-economic analyses of CO_2 liquefaction: Impact of product pressure and impurities. Int J Refrig 2019;103:301–15. https://doi.org/10.1016/J.IJREFRIG.2019.04.011.

[64] Northern lights 2022. https://norlights.com/ (accessed August 18, 2022).

[65] Klemetsrudanlegget and Project CCS Carbon Capture Oslo 2017.https://ccsnorway.com/app/uploads/sites/6/2019/09/fortum_oslo_varme.pdf (accessed August 18, 2022).

[66] Szargut J, Morris DR, Steward FR. Exergy Analysis of Thermal, Chemical, and Metallurgical Processes. 1988.

[67] Singh A, Stéphenne K. Shell Cansolv CO_2 capture technology: Achievement from first commercial plant. Energy Procedia 2014;63:1678–85. https://doi.org/10.1016/j.egypro.2014.11.177.

[68] Ridge B. Testing of Hitachi H3-1 Solvent at the National Carbon Capture Center : Final Report Prepared by : National Carbon Capture Center Wilsonville , AL Hitachi Power Systems America , Ltd . Babcock Hitachi K . K . n.d.

[69] Zheng RF, Barpaga D, Mathias PM, Malhotra D, Koech PK, Jiang Y, et al. A single-component water-lean post-combustion CO_2 capture solvent with exceptionally low operational heat and total costs of capture-comprehensive experimental and theoretical evaluation. Energy Environ Sci 2020;13:4106–13. https://doi.org/10.1039/d0ee02585b.

[70] Tanzer SE, Ramírez A. When are negative emissions negative emissions? Energy Environ Sci 2019;12:1210–8. https://doi.org/10.1039/c8ee03338b.

[71] Stockholm Exergi. Värtaverket, Stockholm Exergi, miljörapport. Stockholm: 2019.

[72] Beiron J. Combined heat and power plant flexibility, Licentiate Thesis. Chalmers University of Technology, Gothenburg 2020. https://research.chalmers.se/en/publication/516671.

[73] State aid for BECCS n.d. https://www.energimyndigheten.se/en/sustainability/carbon-capture-and-storage/state-aid-for-beccs/ (accessed July 8, 2022).

[74] Staffell I, Brett D, Brandon N, Hawkes A. A review of domestic heat pumps n.d. 10.1039/c2ee22653g.